Supported by the Russian Scientific Foundation grant No. 19072-30043
“Computational materials design laboratory

# Density Functional and Dynamical Mean-Field Theory (DFT+DMFT) method and its application to real strongly correlated materials

Vladimir I. Anisimov

*Institute of Metal Physics*
*Ekaterinburg, Russia*

# Contents

## Method formulation:

Dynamical Mean-Field Theory (DMFT)

Wannier functions as localized orbitals basis

Determination of Hamiltonian parameters

“Constrained DFT” calculations for Coulomb interaction parameters

DFT+DMFT calculation scheme

## Results of DFT+DMFT calculations:

**Strongly correlated metal Sr(Ca)$VO_3$**
**Metal-insulator transition in $V_2O_3$**
**Heavy fermions in d-system $Li_2VO_4$**
**Charge transfer insulator NiO**
**Metal-insulator transition with pressure in MnO**
**Correlated covalent insulators FeSi and FeSb2**
**Novel superconductor LaOFeAs**
**Jahn-Teller distortions in $KCuF_3$**
**f-electrons localization in Ce**

# Dynamical Mean-Field Theory

Hubbard model:
Simplest lattice fermions model

Z=4

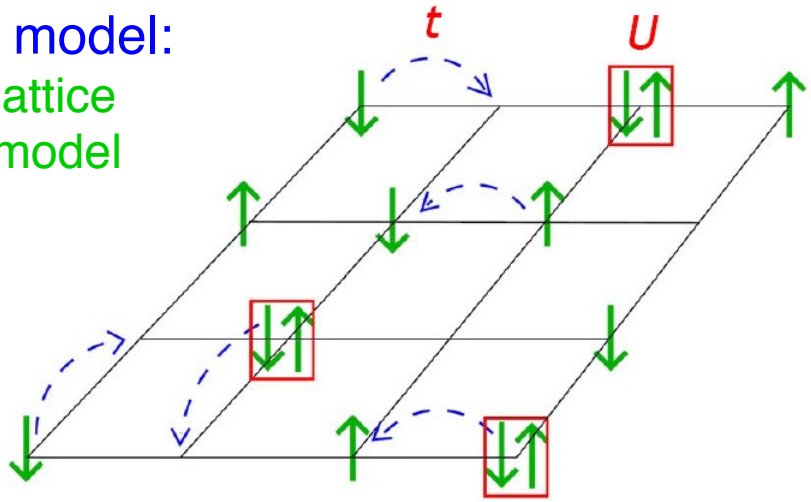


$$H = -t \sum_{\langle \mathbf{i},\mathbf{j}\rangle,\sigma} c^{\dagger}_{\mathbf{i}\sigma} c_{\mathbf{j}\sigma} + U \sum_{\mathbf{i}} n_{\mathbf{i}\uparrow} n_{\mathbf{i}\downarrow}$$

D=2,3: unsolvable many-body problem

- reliable approximations?
- *non-perturbative* energy scale?

Static mean-field (DFT+*U*) does not describe correlated metal and paramagnetic insulator

Gutzwiller (1963)
Hubbard (1963)
Kanamori (1963)

DFT DFT+*U* (AF)

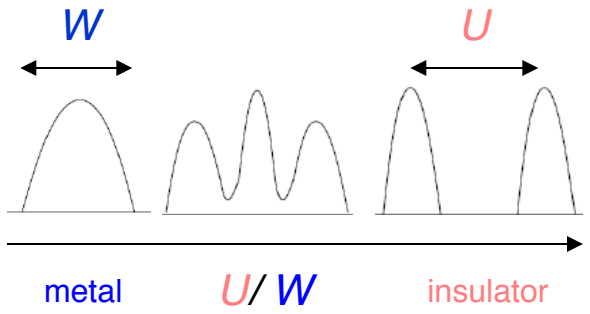


$$\langle n_{\mathbf{i}\uparrow} n_{\mathbf{i}\downarrow} \rangle \neq \langle n_{\mathbf{i}\uparrow} \rangle \langle n_{\mathbf{i}\downarrow} \rangle$$

**Correlation phenomena:**
Metal-insulator transition
Ferromagnetisms,...

# Dynamical Mean-Field Theory

Single-impurity Anderson Model:

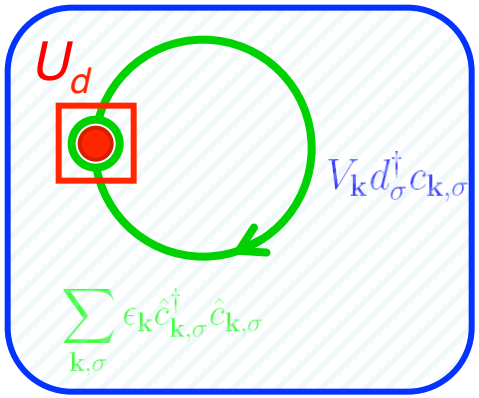


$$\hat{H}_{SIAM} = \sum_{\mathbf{k},\sigma} \epsilon_{\mathbf{k}} \hat{c}^\dagger_{\mathbf{k},\sigma} \hat{c}_{\mathbf{k},\sigma} + U \hat{n}_{d\uparrow} \hat{n}_{d\downarrow} + \sum_{\mathbf{k},\sigma} (V_{\mathbf{k}} d^\dagger_\sigma c_{\mathbf{k},\sigma} + h.c.)$$

many-body problem: solve with QMC, NRG,…

- Characteristic 3-peak structure
- *non-perturbative* energy scale ("Kondo physics")

Non-interacting conduction (*s*-) electrons

+

Single *d*-orbital ("impurity") with **interaction** *U*

+

*s,d*-hybridization

SIAM spectral function:

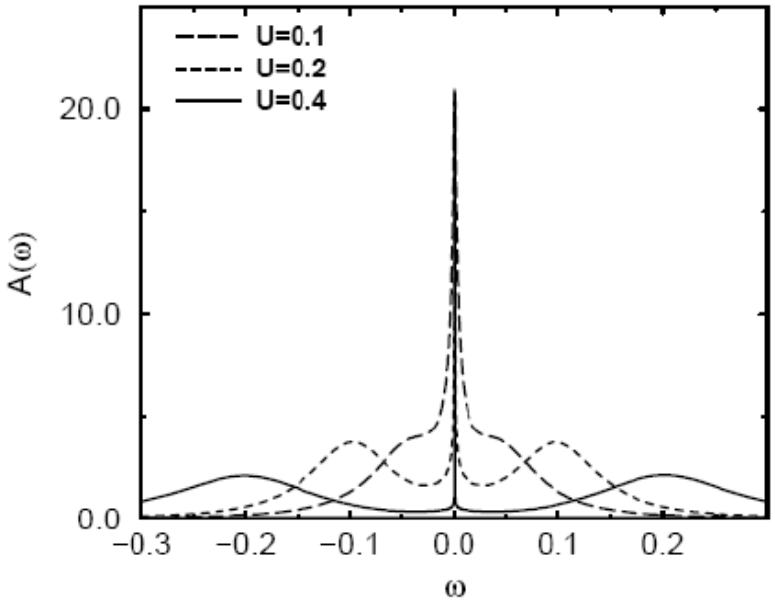

# Dynamical Mean-Field Theory

Mapping impurity Anderson model on lattice Hubbard model

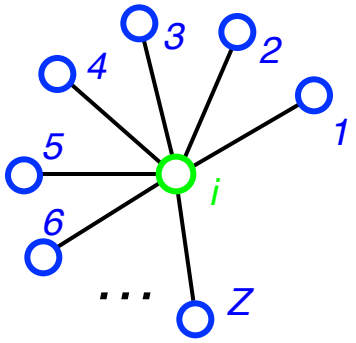


Metzner,Vollhardt (1989)

$d \to \infty$
$Z \to \infty$

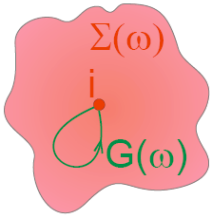


"single-impurity Anderson model" + self-consistency

Georges and Kotliar (1992)

Hubbard model:

$$H = -t \sum_{\langle \mathbf{i},\mathbf{j} \rangle,\sigma} c^{\dagger}_{\mathbf{i}\sigma} c_{\mathbf{j}\sigma} + U \sum_{\mathbf{i}} n_{\mathbf{i}\uparrow} n_{\mathbf{i}\downarrow}$$

- proper time resolved treatment of local electronic interactions
- includes all many-body correlations !

*dynamic* mean-field (hybridization function):

$$\Delta(\omega) = \sum_{\mathbf{k}} \frac{|V_{\mathbf{k}}|^2}{\omega - \epsilon_{\mathbf{k}}}$$

self-consistency condition:

$$G[\Delta(\omega)] = \sum_{\mathbf{k}} \{\omega - \Sigma[\Delta(\omega)] - t_{\mathbf{k}}\}^{-1}$$

$$\Sigma[\Delta(\omega)] \equiv \Delta(\omega) - G^{-1}(\Delta(\omega)) + \omega$$

Effective impurity model defined by hybridization function is solved with an "impurity" solver, e.g., QMC, NRG, ED,…

# Including material specific details

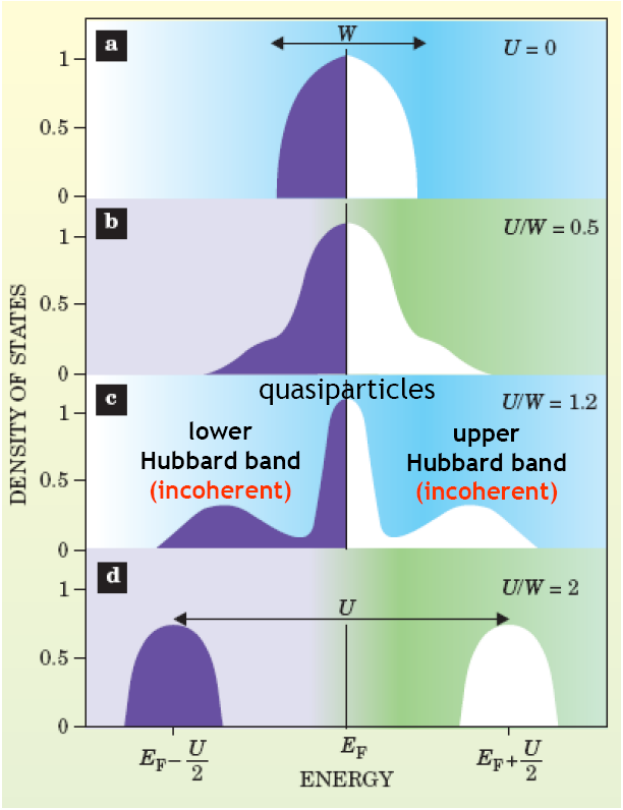


Anisimov *et al.* (1997)
Lichtenstein, Katsnelson (1998)
Kotliar, Vollhardt (2004)

Model Hamiltonians:
- input parameters (*t, U, …*) unknown
- systematic many-body approach

**DFT+DMFT**

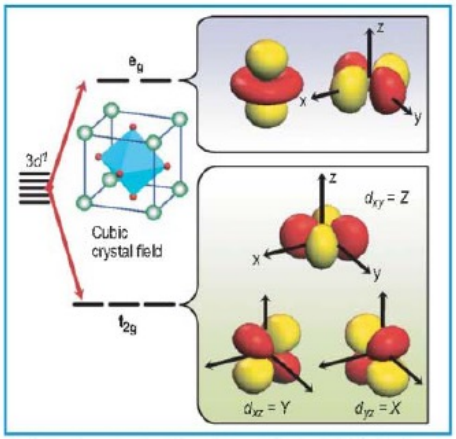


Density Functional Theory:
- material specific: *"ab initio"*
- fails for strong correlations

- DFT band structure: $\varepsilon_{lml'm'}(k) \rightarrow \hat{H}_{LDA}$
- + Coulomb *U* $\rightarrow \hat{H}_{LDA+corr}$
- solve $\hat{H}_{LDA+corr}$ by DMFT

# Wannier functions as orbitals basis set

## Wannier functions in real space [1]:

$$W_i(\mathbf{r}-\mathbf{T}) = \sum_{\mathbf{k}} e^{-i\mathbf{k}\mathbf{T}} \langle \mathbf{r} | \psi_{i\mathbf{k}} \rangle$$

← Bloch functions

**Advantages of Wannier function basis set:**

<Explicit form of the orbitals forming complete basis set

? Localized orbitals

? Orbitals are centered on atoms

} like in Hubbard model

**Uncertainty of WF definition for a many-band case:**

$$|\psi_{i\mathbf{k}}\rangle = \sum_j U_{ji}^{(\mathbf{k})} |\psi_{j\mathbf{k}}\rangle$$

Unitary matrix

[1] G.H. Wannier, Phys. Rev. **52**, 192 (1937)

# Wannier functions and projection

**WF in k-space –** projection of the set of trial functions [2] (atomic orbitals) into Bloch functions subspace :

$$|\widetilde{W}_{n\mathbf{k}}\rangle = \sum_{i=N_1}^{N_2} |\psi_{i\mathbf{k}}\rangle\langle\psi_{i\mathbf{k}}|\phi_n\rangle$$

**Bloch functions in DFT basis (LMTO or plane waves):**

$$\psi_{i\mathbf{k}}(\mathbf{r}) = \sum_j c_{ji}(\mathbf{k})\phi_j^{\mathbf{k}}(\mathbf{r})$$

Eigenvector element

Bloch sums of LMTO orbitals

$$|\widetilde{W}_{n\mathbf{k}}\rangle = \sum_{i=N_1}^{N_2}\sum_j c_{ji}(\mathbf{k})c_{ni}^{\star}(\mathbf{k})|\phi_j^{\mathbf{k}}\rangle = \sum_j \tilde{b}_{jn}^{\mathbf{k}}|\phi_j^{\mathbf{k}}\rangle$$

**coefficients** of WF expansion in LMTO-orbitals:

$$\tilde{b}_{jn}^{\mathbf{k}} = \sum_{i=N_1}^{N_2} c_{ji}(\mathbf{k})c_{ni}^{\star}(\mathbf{k})$$

[2] D.Vanderbildt et al, Phys. Rev.B **56**, 12847 (1997)

# Example of WF in real space

WF basis set for V-3d ($t_{2g}$) subband of $SrVO_3$: *XY, XZ, YZ* - orbitals

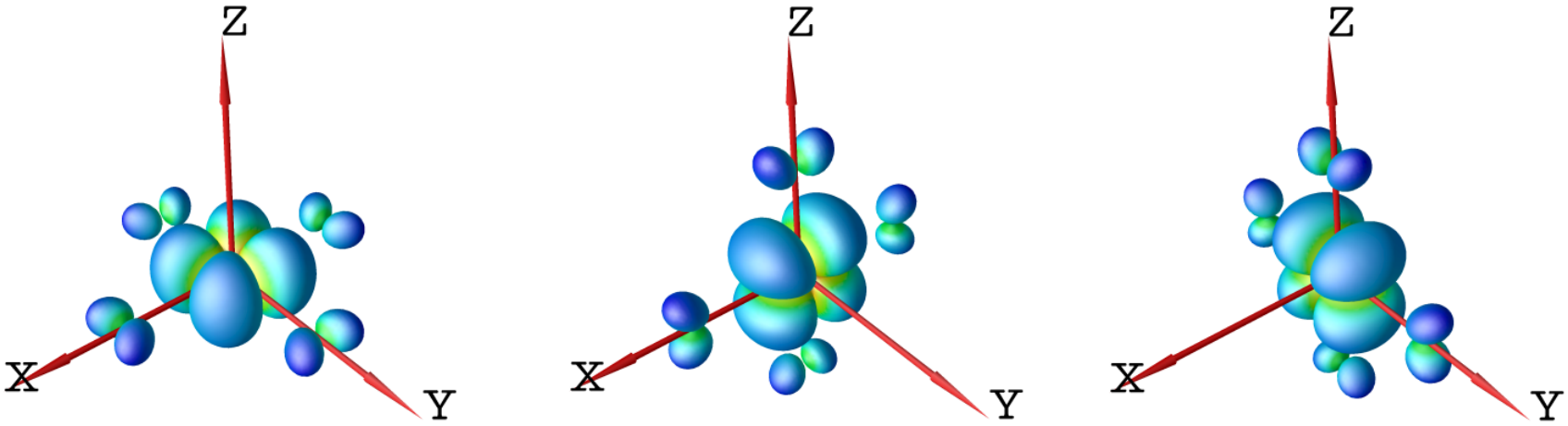

# d-xy WF for NiO

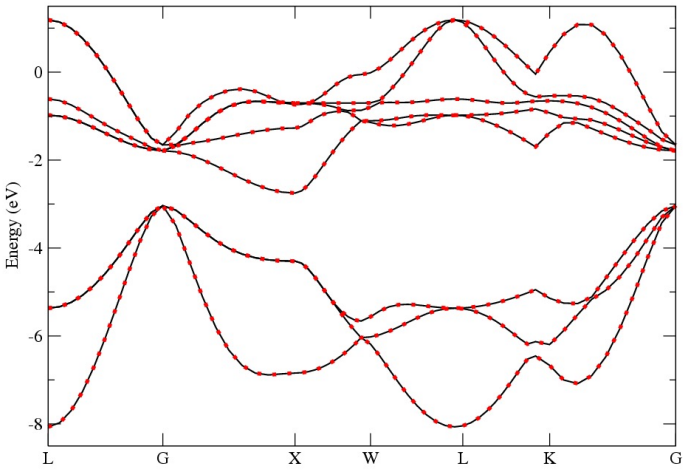


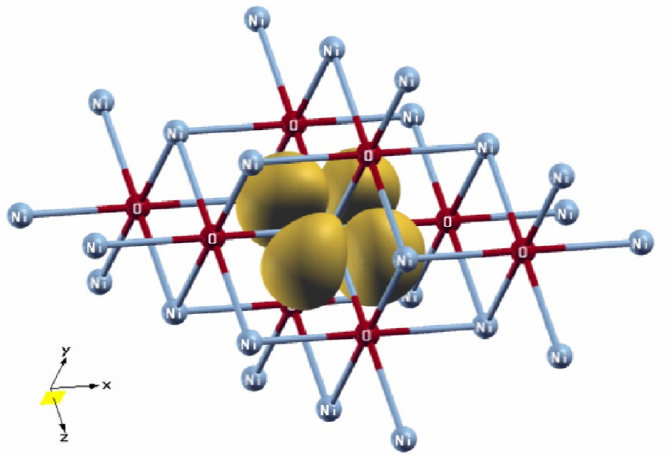


Full bands projection

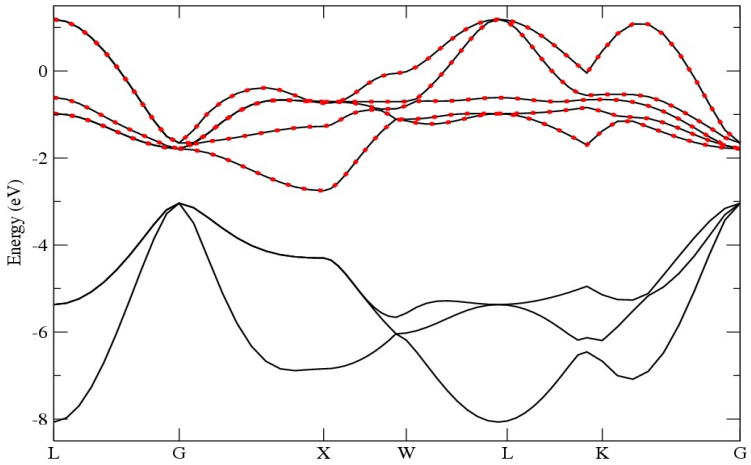


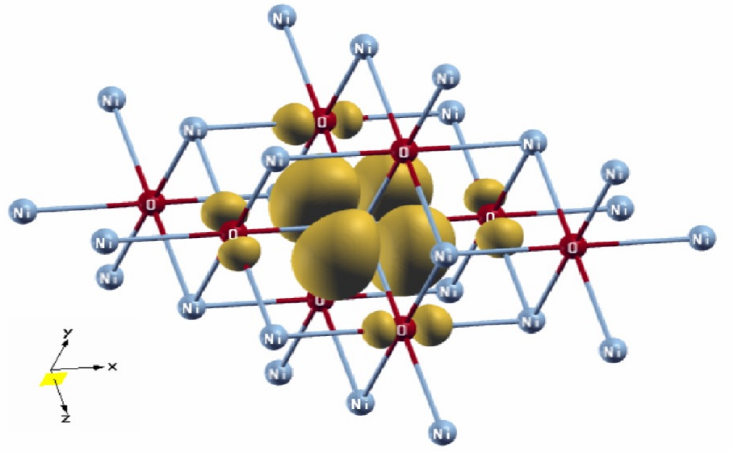


d-bands only projection

Dm.Korotin et al, Europ. Phys. J. B 65, 91 (2008).

# WF for stripe phase in cuprates

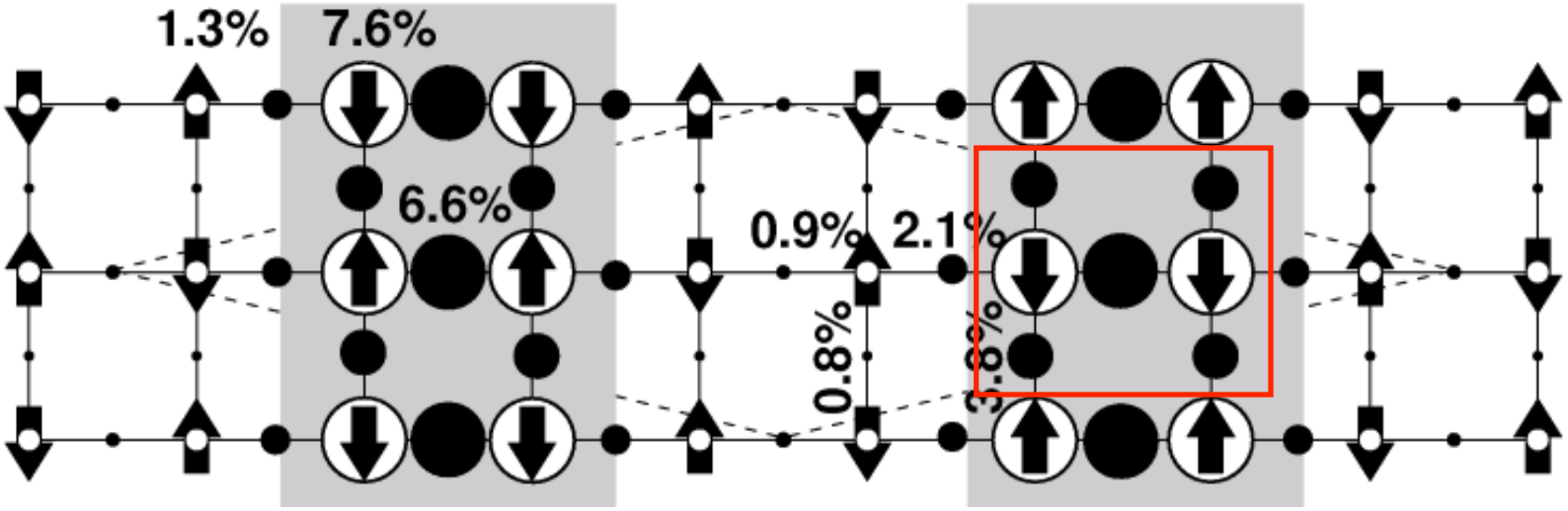


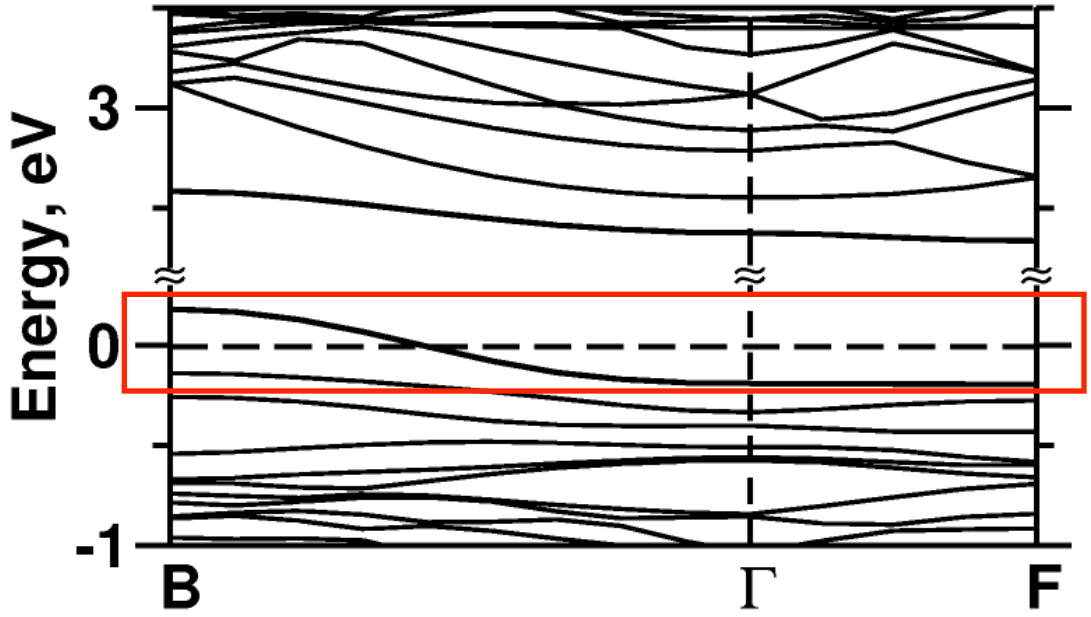


$La_{7/8}Sr_{1/8}CuO_4$

Half-filled band

V.Anisimov et al, Phys. Rev. B 70, 172501 (2004)

# WF for stripe phase in cuprates

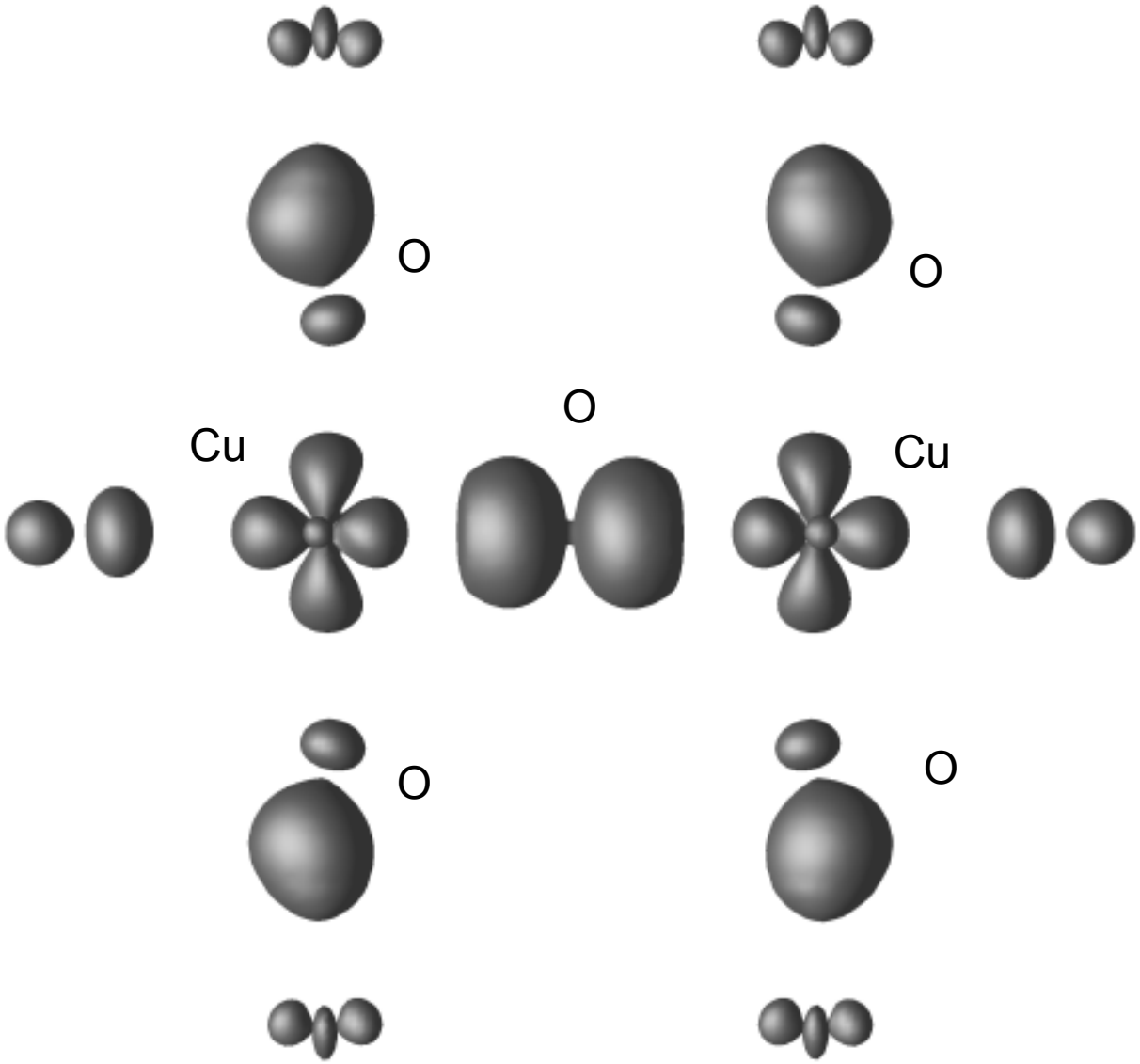

# Projection procedure for Hamiltonian

**Matrix elements of projected Hamiltonian:**

$$\widetilde{H}^{WF}_{nm}(\mathbf{k}) = \langle \widetilde{W}_{n\mathbf{k}} | \Big( \sum_{i\mathbf{k}'} |\psi_{i\mathbf{k}'}\rangle \epsilon_i(\mathbf{k}') \langle \psi_{i\mathbf{k}'}| \Big) | \widetilde{W}_{m\mathbf{k}} \rangle = \sum_{i=N_1}^{N_2} c_{ni}(\mathbf{k}) c^{\star}_{mi}(\mathbf{k}) \epsilon_i(\mathbf{k})$$

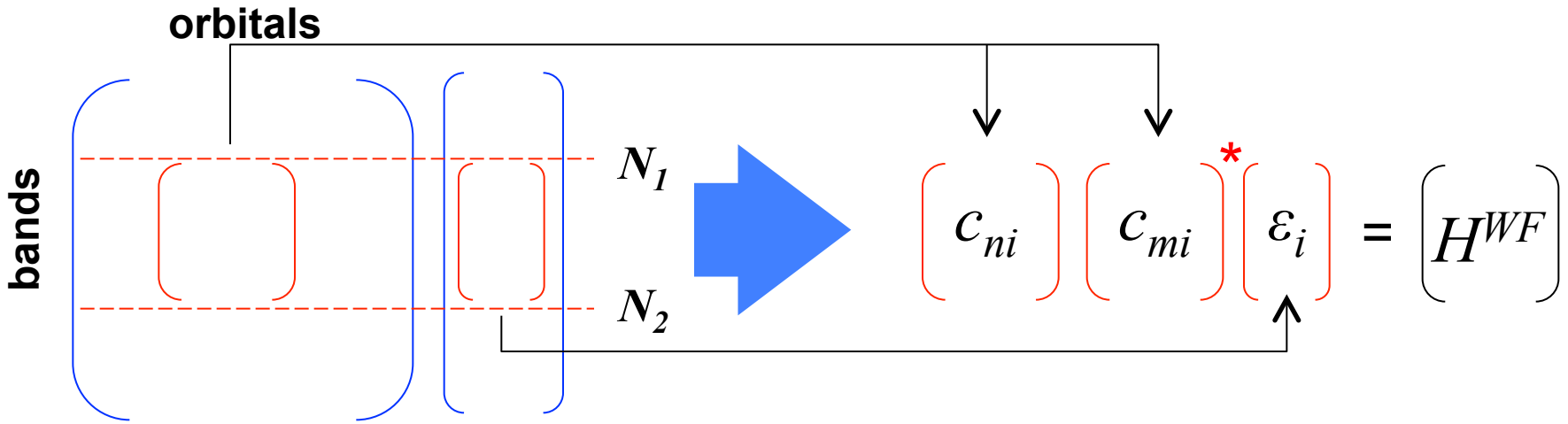


**LMTO Eigenvectors, Eigenvalues**

# Projection results for $SrVO_3$

Full-orbital Hamiltonian

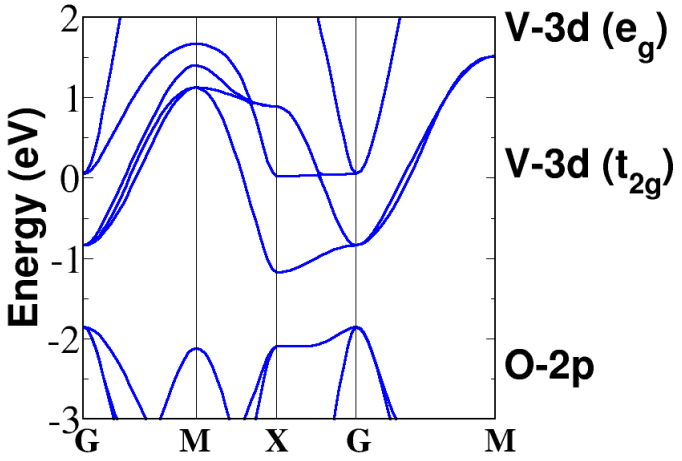


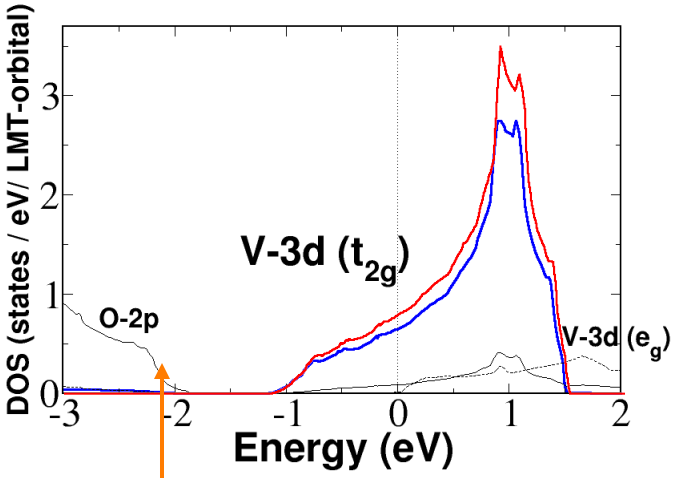


Projected Hamiltonian

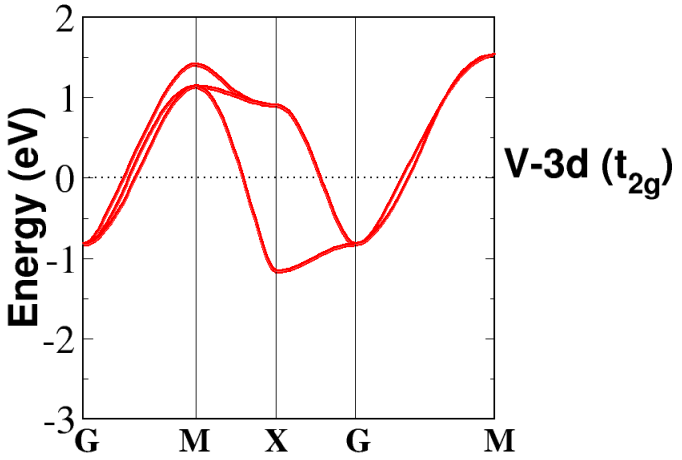


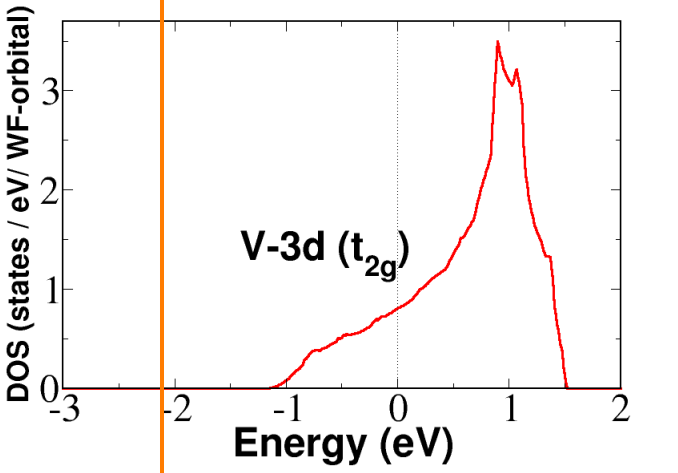


Eigenvalues of full-orbital and projected Hamiltonians are the same

Projected Hamiltonian DOS corresponds to the total DOS of full-orbital Hamiltonian

# Constrain DFT Calculation of U

**Matrix of projected Hamiltonian in real space:**

$$H_{nm}^{WF} = \langle W_n^{\mathbf{0}} | \Big( \sum_{\mathbf{k}} \sum_{i=N_1}^{N_2} |\psi_{i\mathbf{k}}\rangle \epsilon_i(\mathbf{k}) \langle \psi_{i\mathbf{k}}| \Big) |W_m^{\mathbf{0}}\rangle = \sum_{\mathbf{k}} \sum_{i=N_1}^{N_2} \bar{c}_{ni}(\mathbf{k}) \bar{c}_{mi}^{\star}(\mathbf{k}) \epsilon_i(\mathbf{k})$$

**Density matrix operator:**

$$Q_{nm}^{WF} = \langle W_n^{\mathbf{0}} | \Big( \sum_{\mathbf{k}} \sum_{i=N_1}^{N_2} |\psi_{i\mathbf{k}}\rangle \theta(\epsilon_i(\mathbf{k}) - E_f) \langle \psi_{i\mathbf{k}}| \Big) |W_m^{\mathbf{0}}\rangle = \sum_{\mathbf{k}} \sum_{i=N_1}^{N_2} \bar{c}_{ni}(\mathbf{k}) \bar{c}_{mi}^{\star}(\mathbf{k}) \theta(\epsilon_i(\mathbf{k}) - E_f)$$

**Energy of *n*-th WF:** $E_n = H_{nn}^{WF}$

**Occupation of *n*-th WF:** $Q_n = Q_{nn}^{WF}$

**Coulomb interaction**

$$U \equiv \frac{\partial E_n}{\partial Q_n}$$

# DFT+DMFT calculations scheme

**Local Green function:**

$$G^{loc}_{n,n'}(\varepsilon) = \frac{1}{V_{IBZ}} \int_{IBZ} d\mathbf{k} \left( \left[ (\varepsilon + E_f^{(N)}) 1 - H_0^{WF}(\mathbf{k}) - \Sigma(\varepsilon) \right]^{-1} \right)_{n,n'}$$

**Dyson equation defines bath Green function:**

$$\mathcal{G}^{-1} = (G^{loc})^{-1} + \Sigma$$

**Self-consistent condition:**

$$G^{loc} = G^{imp} \Rightarrow \Sigma_{new}$$

**Impurity problem defined bath Green function is solved by QMC**

# Strongly correlated metal $SrVO_3$

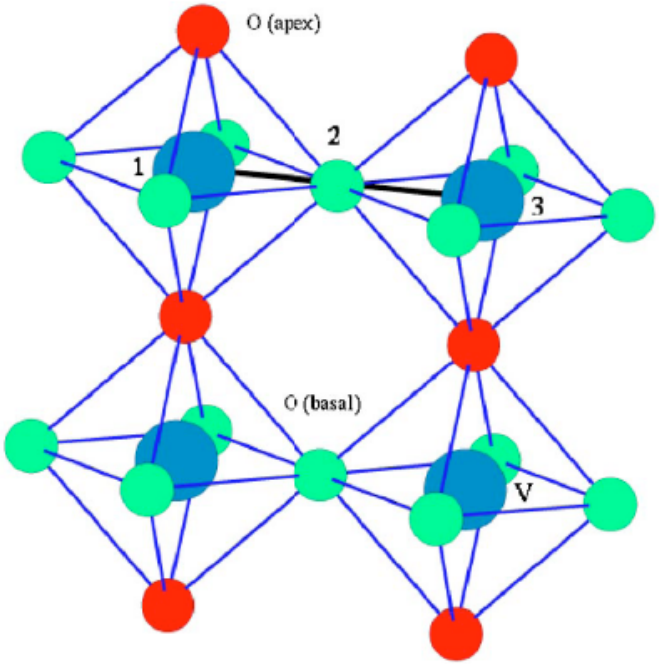


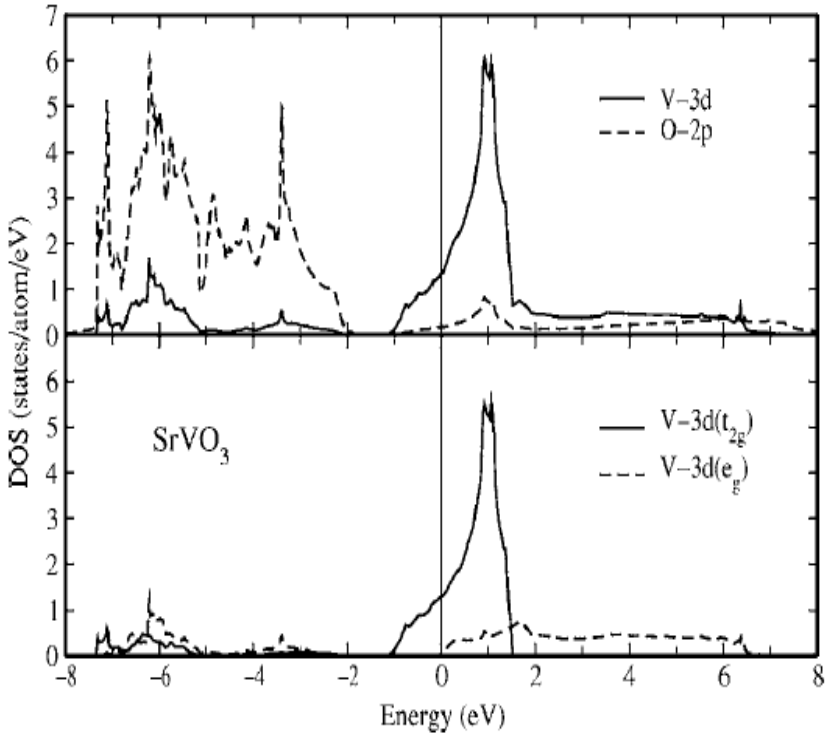


$V^{+4}$ ($d^1$) ion in cubic perovskite crystal structure

One electron in partially filled $t_{2g}$ band

I.Nekrasov et al, Phys. Rev. B **72**, 155106 (2005), Phys. Rev. B **73**, 155112 (2006)

# Strongly correlated metal $SrVO_3$

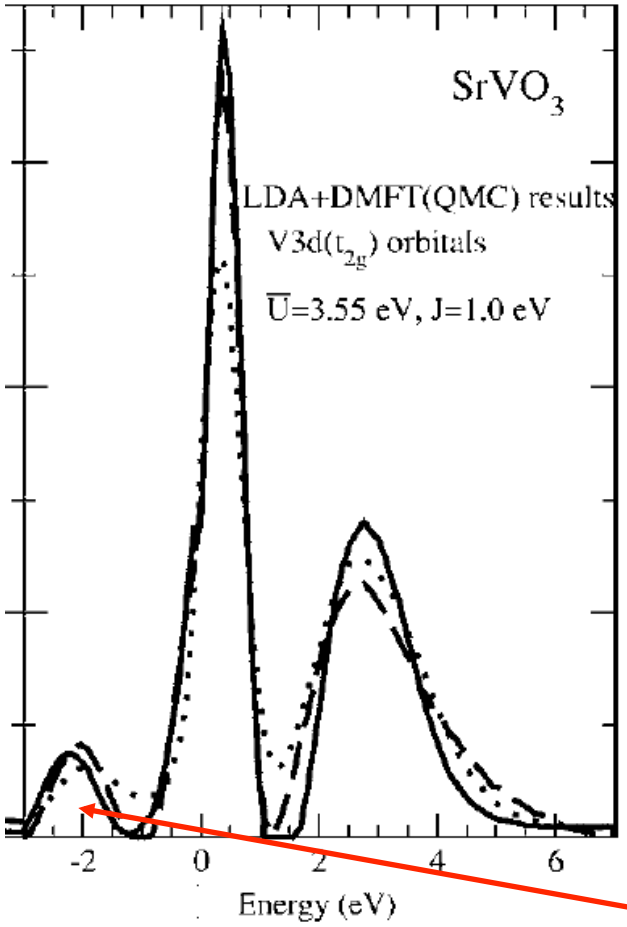


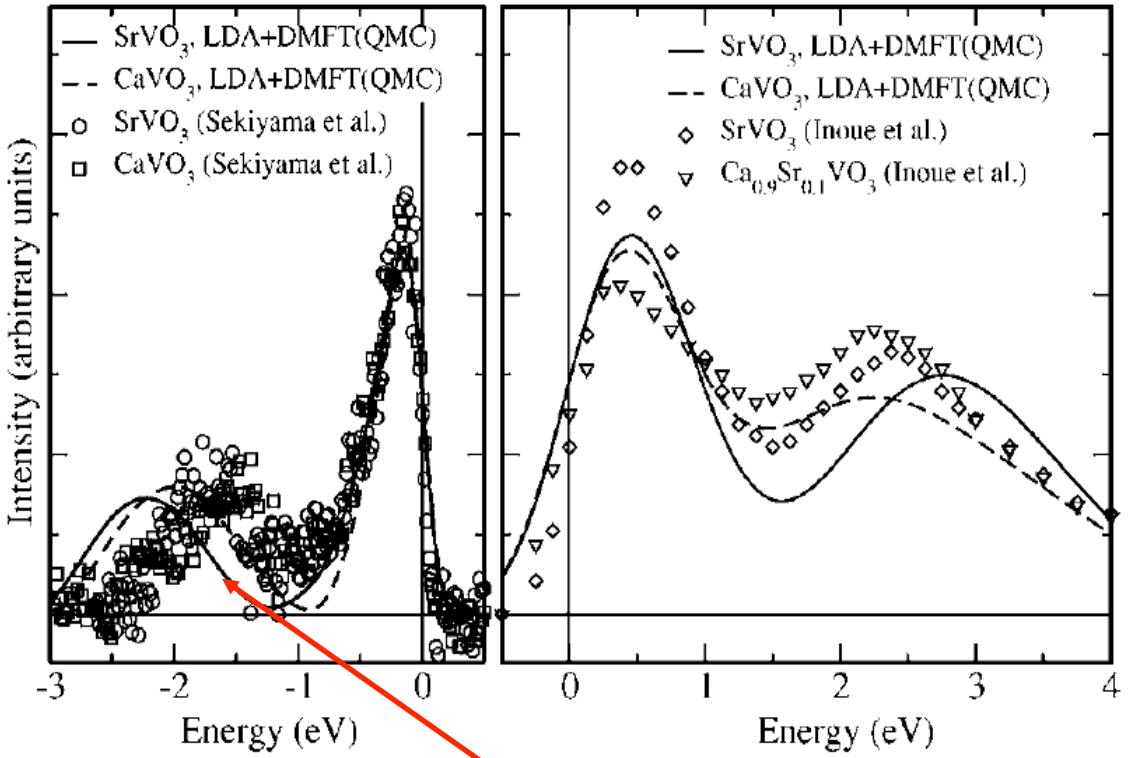


Strongly correlated metal with pronounced Lower Hubbard band (LHB)

# Strongly correlated metal $SrVO_3$

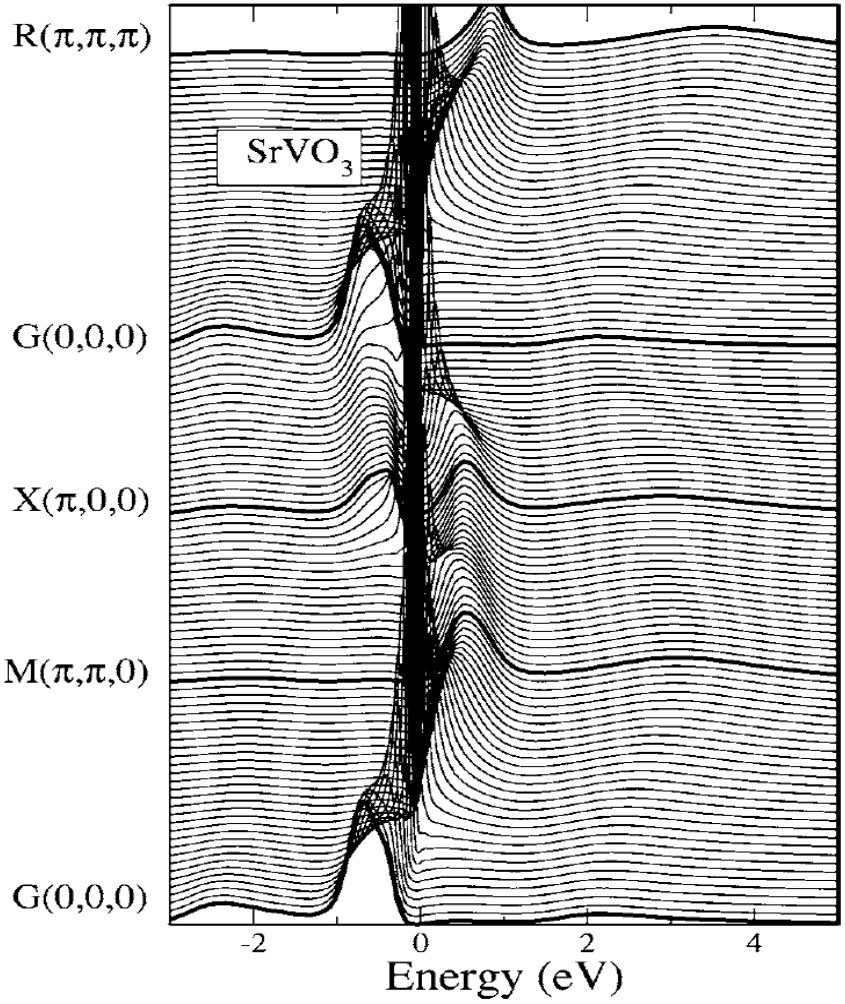


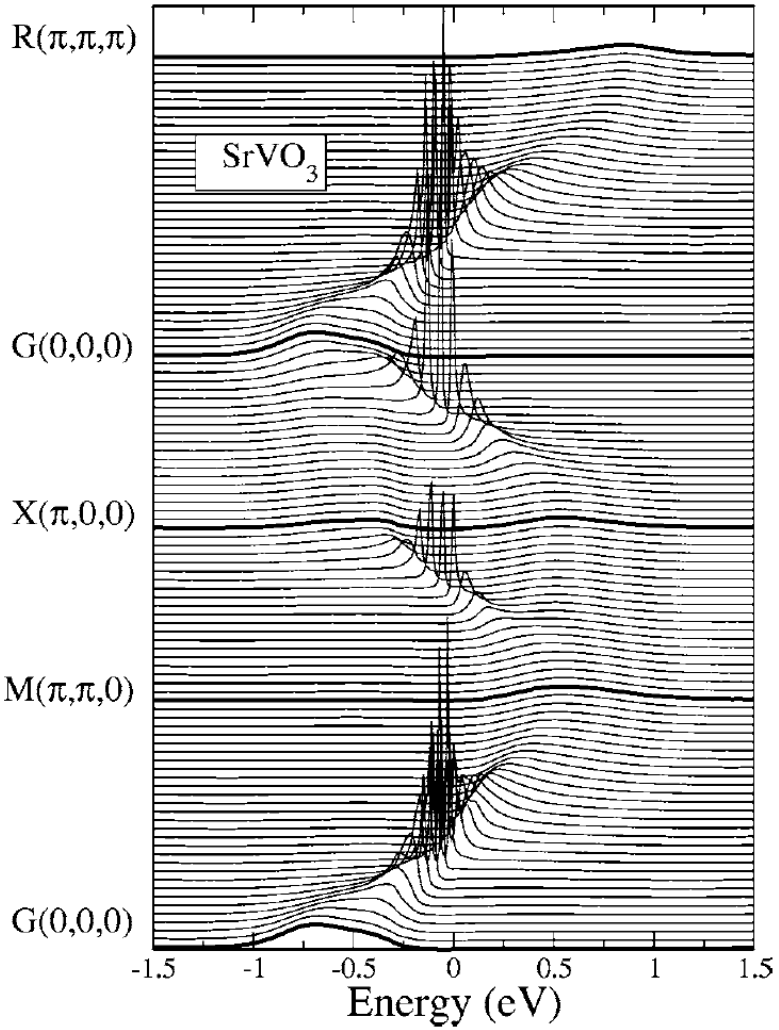


$$\text{Spectral function } A(k,\omega) = -\frac{1}{\pi}\,\mathrm{Im}\,\mathrm{Tr}\left[\omega - \Sigma(\omega) - H_0(k)\right]^{-1}$$

# Strongly correlated metal $SrVO_3$

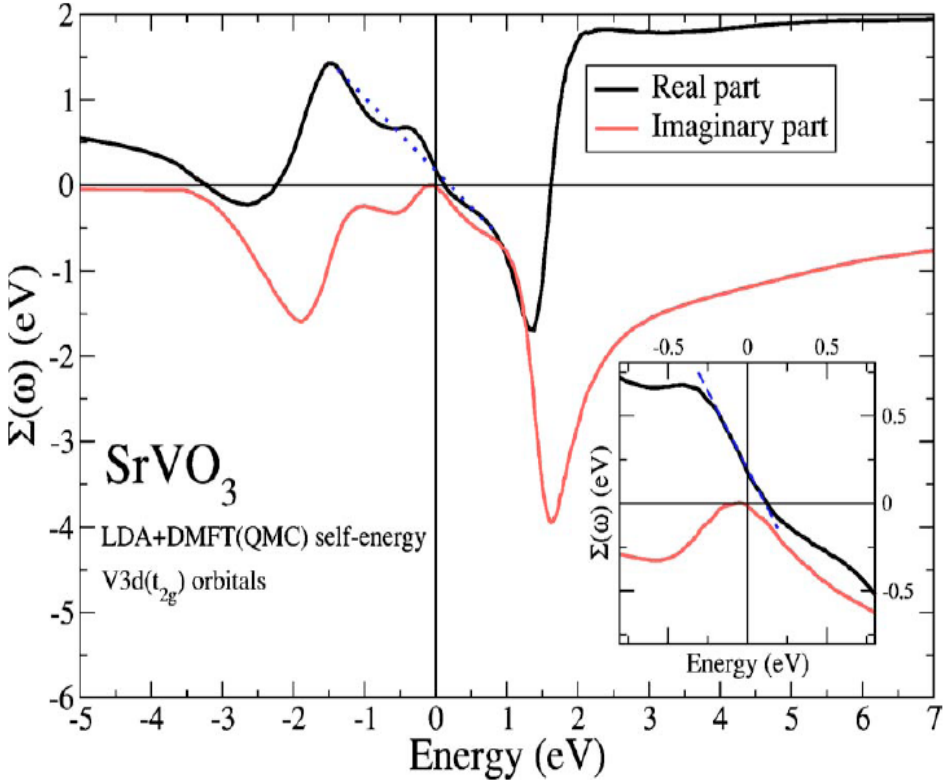


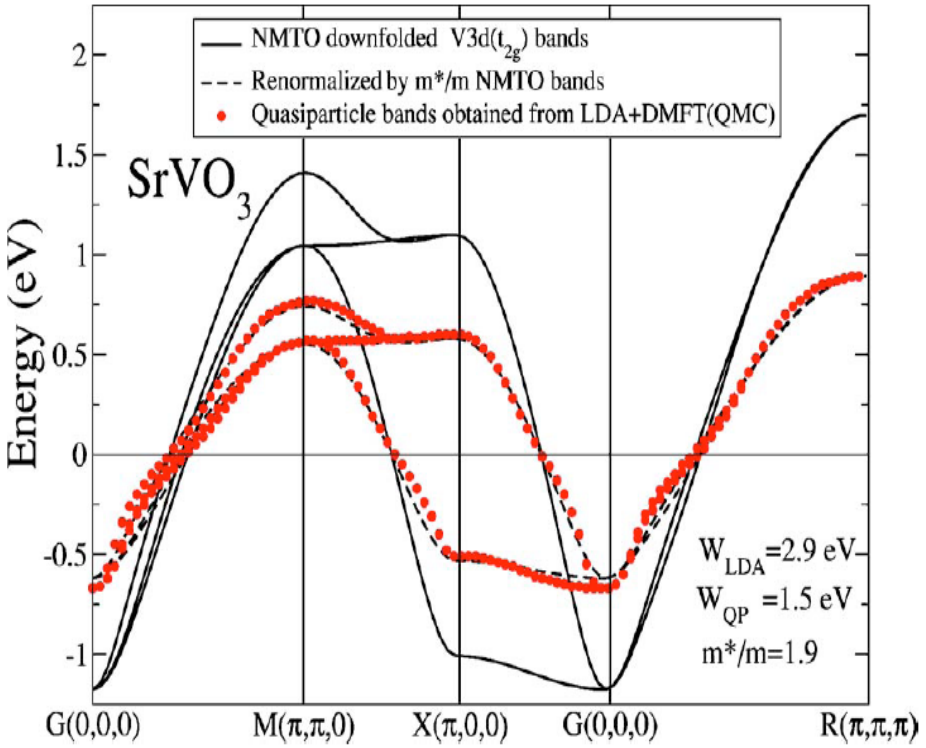


Effective electron mass

$$\frac{m^*}{m} = 1 - \frac{\partial\, \mathrm{Re}\,\Sigma(\omega)}{\partial\omega}\Big|_{\omega=0} \approx 2$$

Bands narrowing

$$\tilde{\varepsilon}\,(\mathrm{k}) = \left(\frac{m^*}{m}\right)^{-1} \varepsilon_0(k)$$

# Mott insulator $V_2O_3$

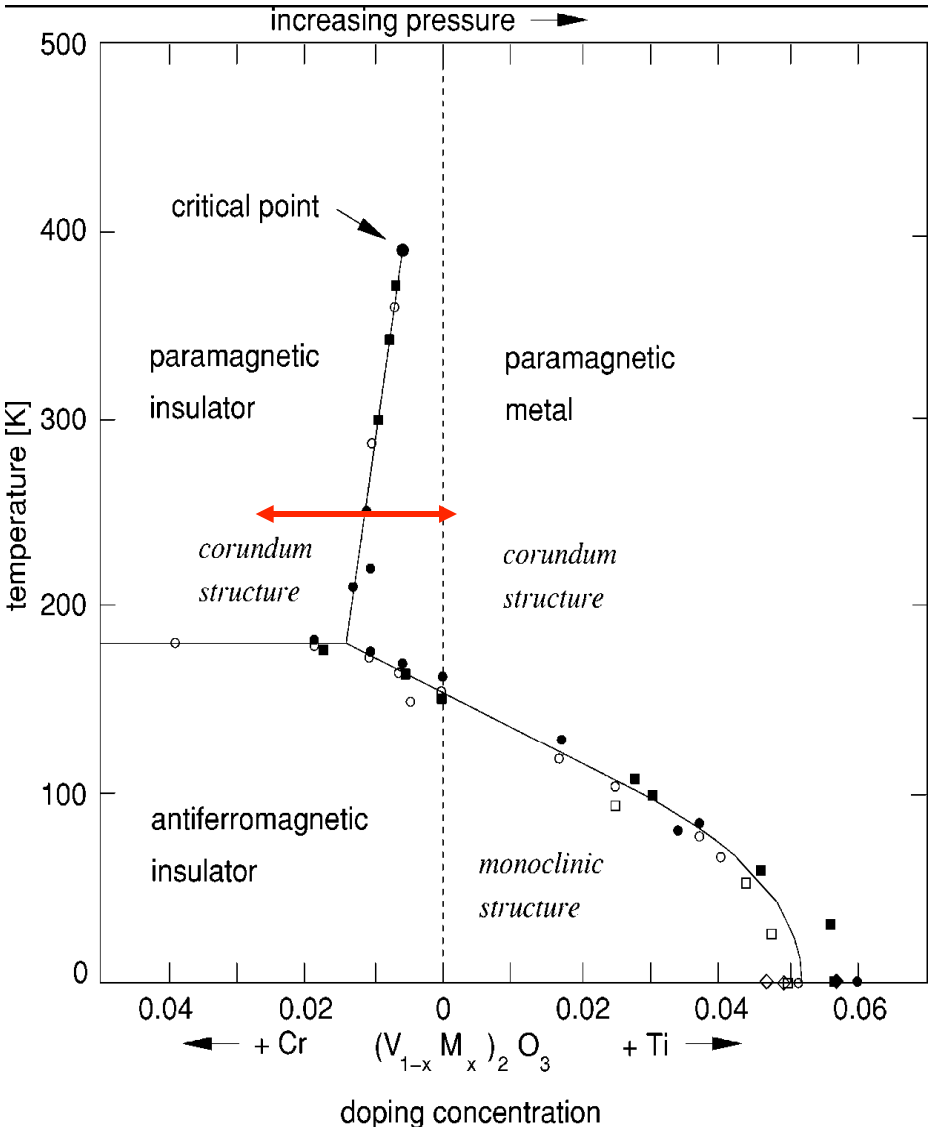


Prototypical Mott insulator.
Iso-structural paramagnetic metal to paramagnetic insulator transition with small volume change due to chemical negative pressure.

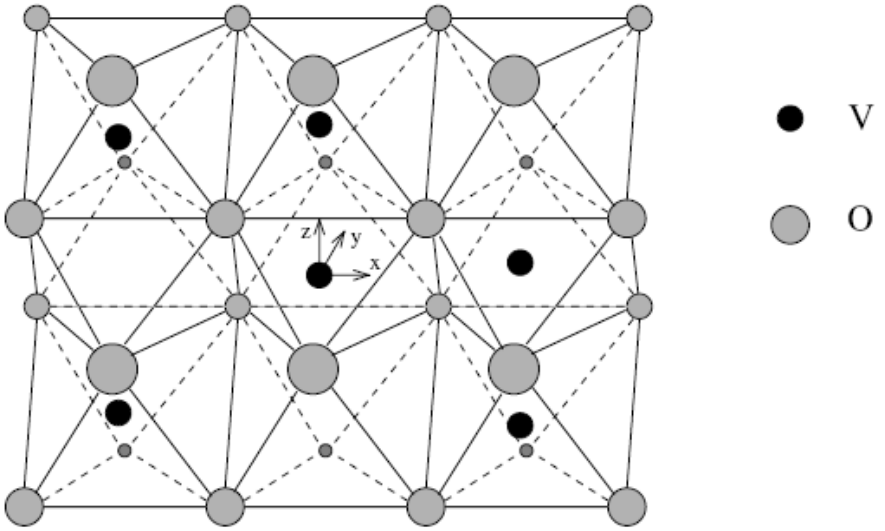

# Mott insulator $V_2O_3$

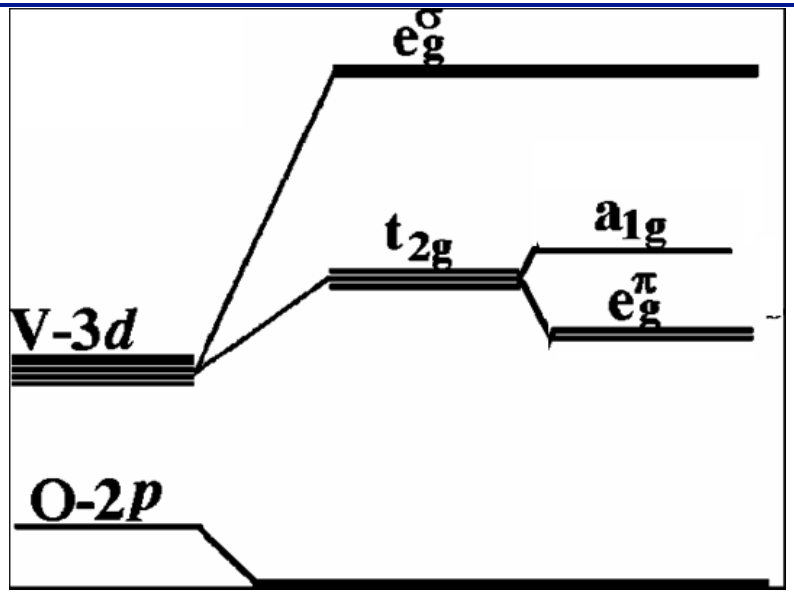


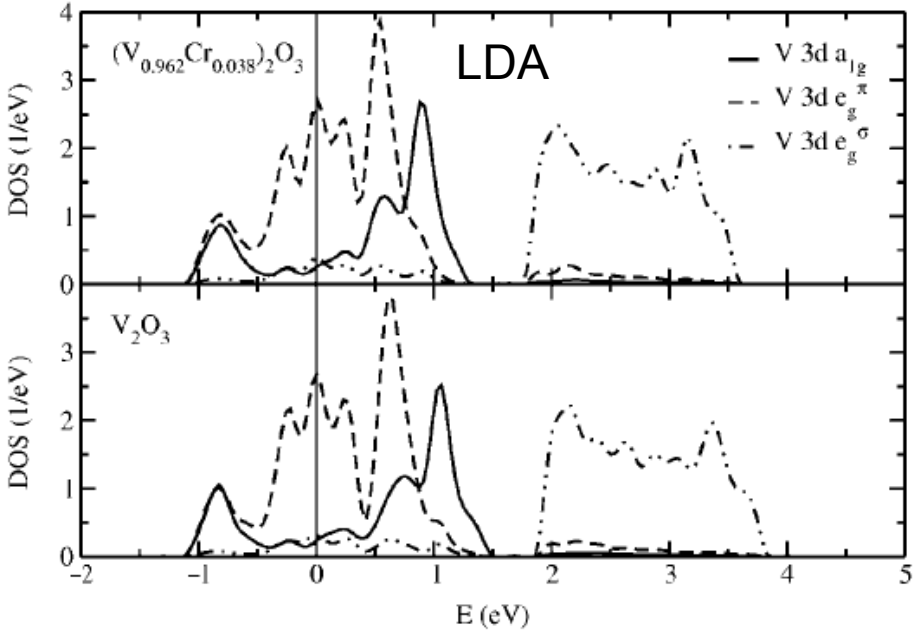


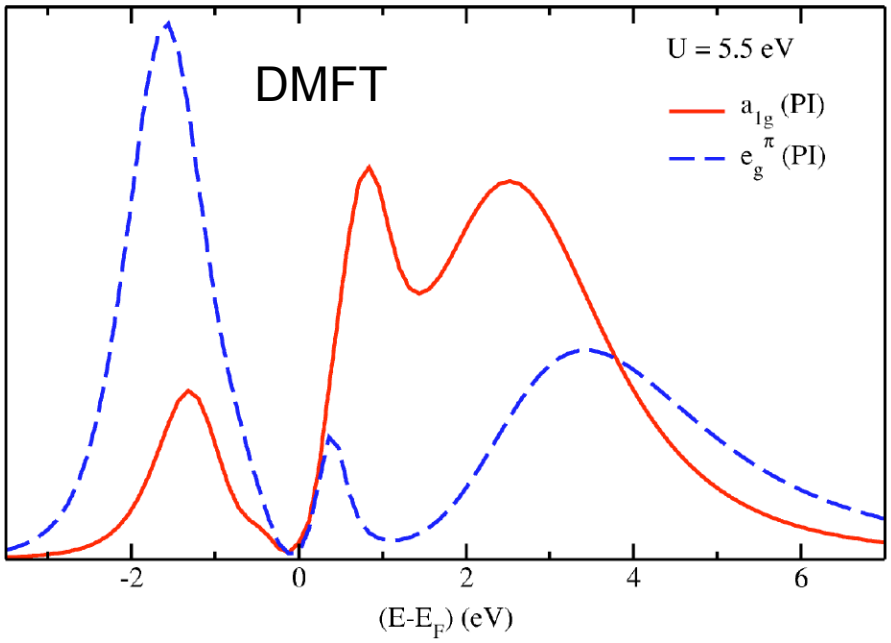


$V^{+3}$ ($d^2$) ion in trigonal symmetry corundum crystal structure.
Two electrons in $t_{2g}$ band (W~2.5 eV).
Trigonal crystal field splitting ~0.3 eV leads to orbital polarization in DMFT

# Mott insulator $V_2O_3$

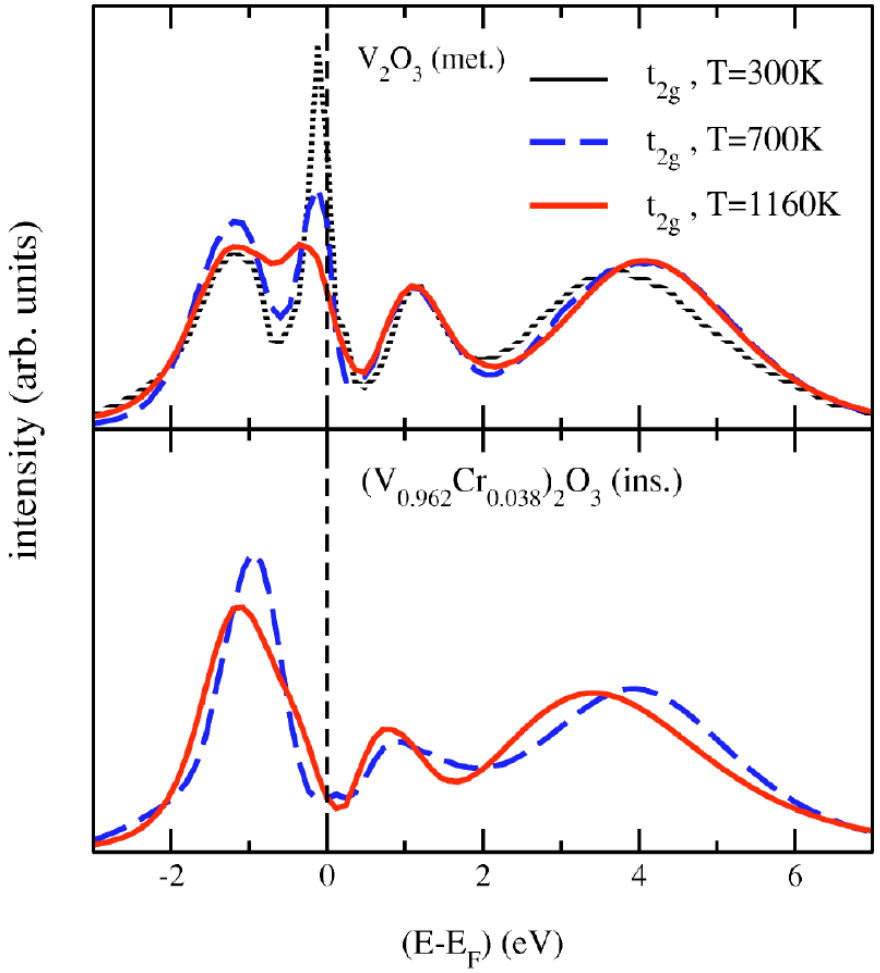


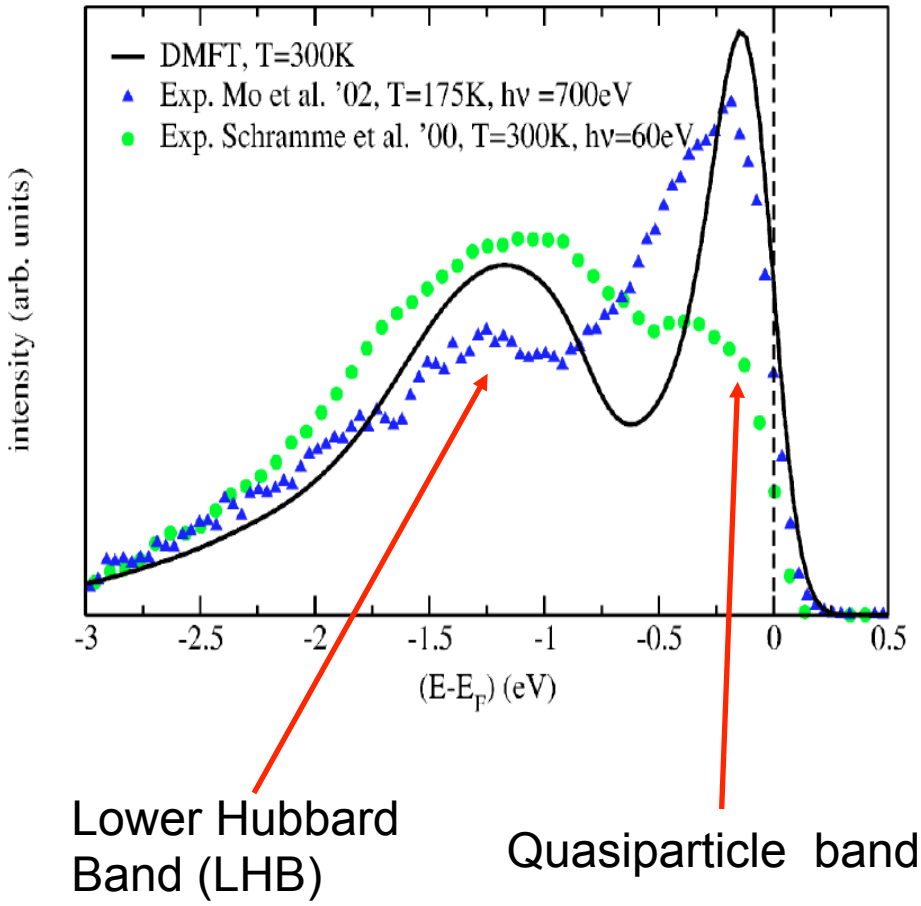


Paramagnetic metal to paramagnetic insulator transition with small change in corundum crystal structure parameters

K.Held et al, Phys. Rev. Lett. 86, 5345 (2001), G.Keller et al, Phys. Rev. B 70, 205116 (2004)

# Heavy fermions material $LiV_2O_4$

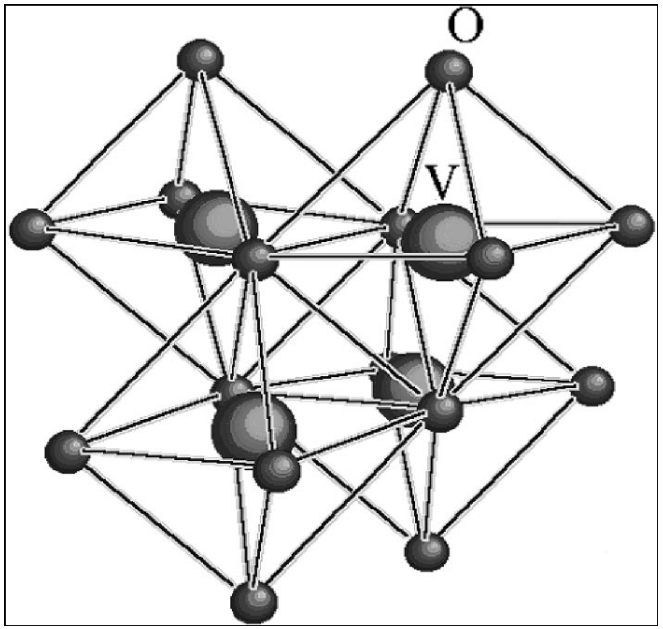


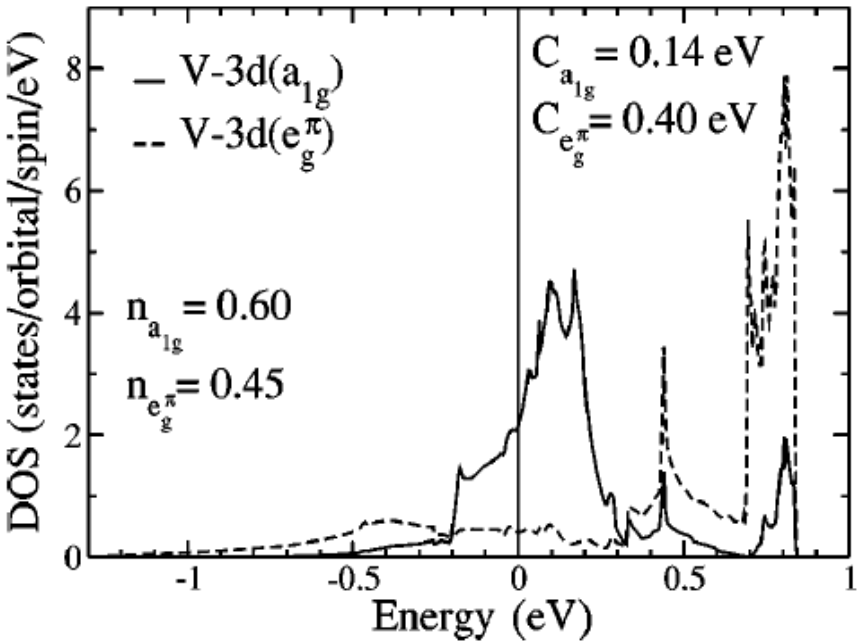


Heavy-fermions without f-electrons:
linear specific heat coefficient
g=420 mJ/molK$^2$,
effective electron mass $m^*/m$ =25
below $T_K$ ~28 K

Cubic spinel crystal structure
with local trigonal symmetry

# Heavy fermions material $LiV_2O_4$

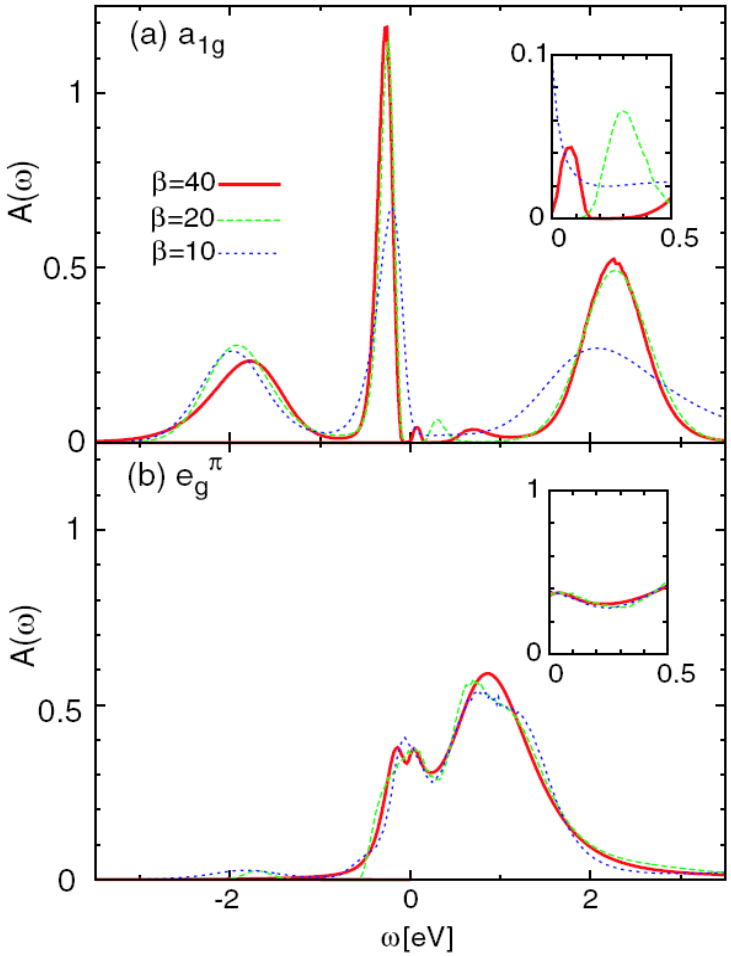


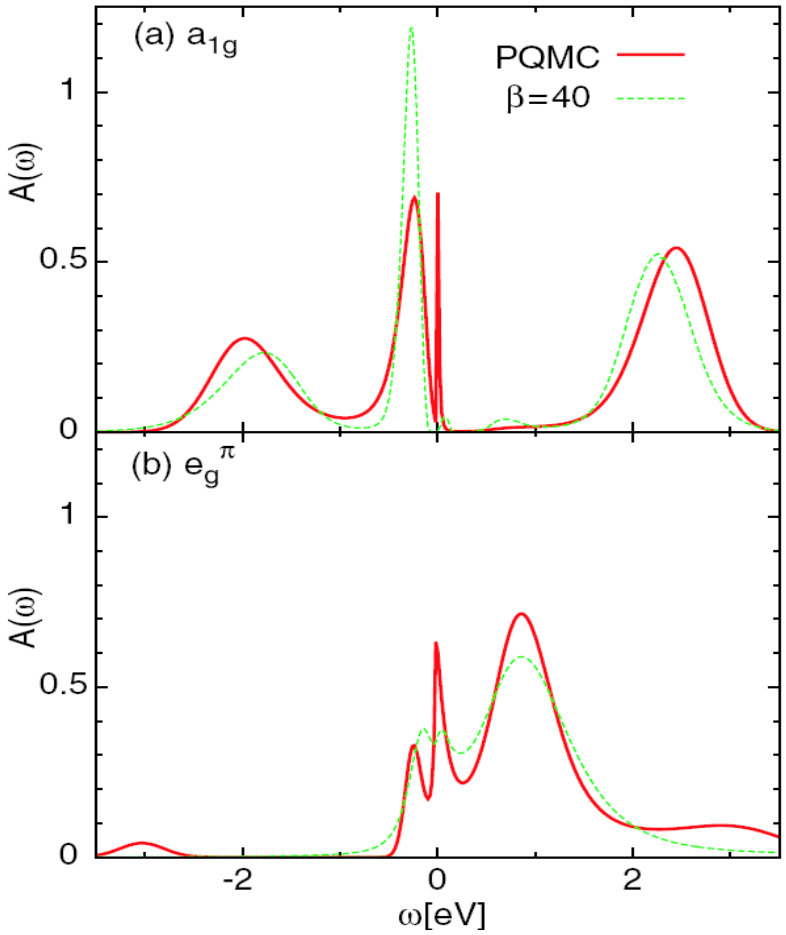


Sharp quasiparticle peak above the Fermi for T=0 limit (PQMC)

R.Arita et al, Phys. Rev. Lett. 98, 166402 (2007)

# Heavy fermions material $LiV_2O_4$

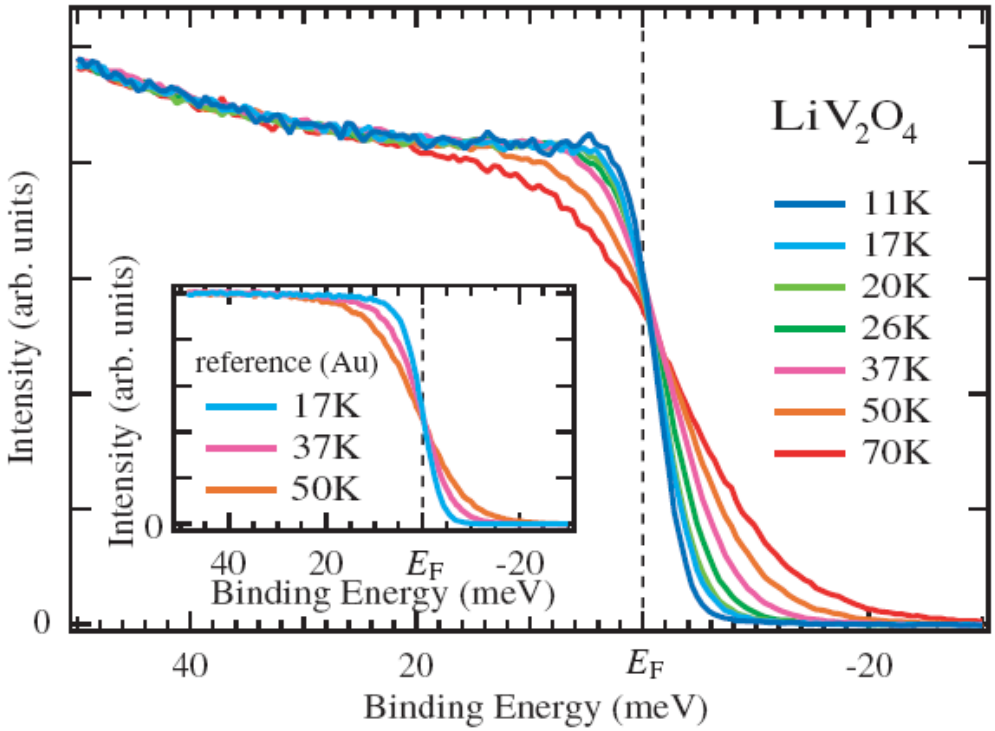


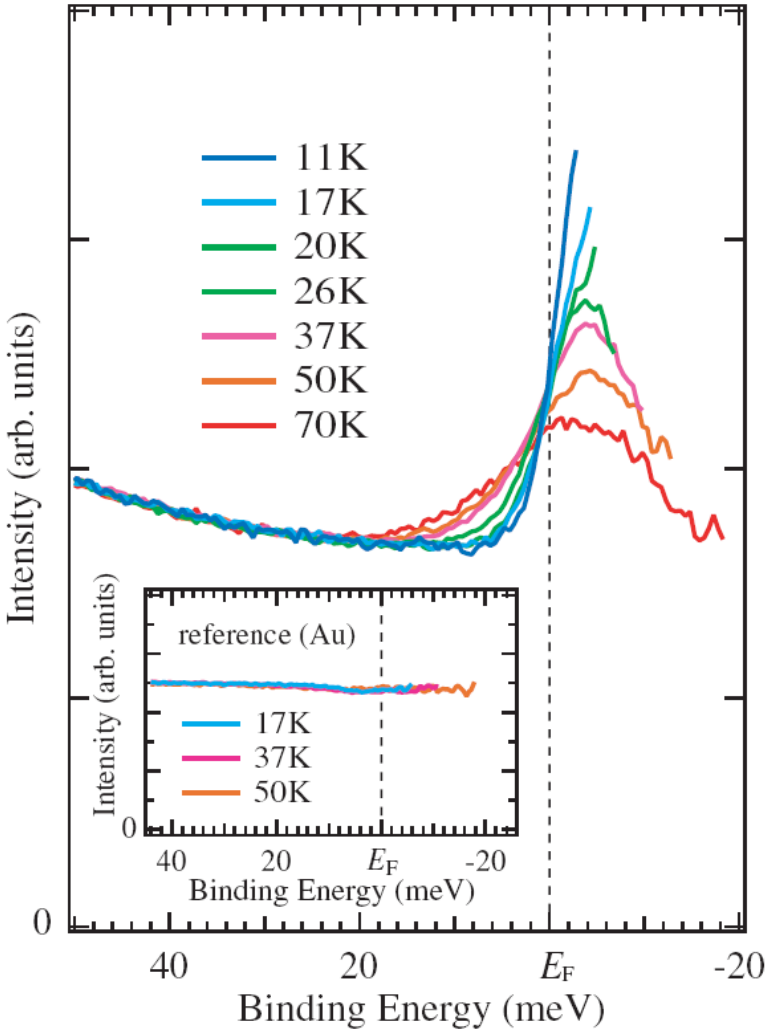


XPS => Quasiparticle peak 10 meV width
4 meV above the Fermi

A. Shimoyamada, et al, Phys. Rev. Lett. 96, 026403 (2006)

# Charge transfer insulator NiO

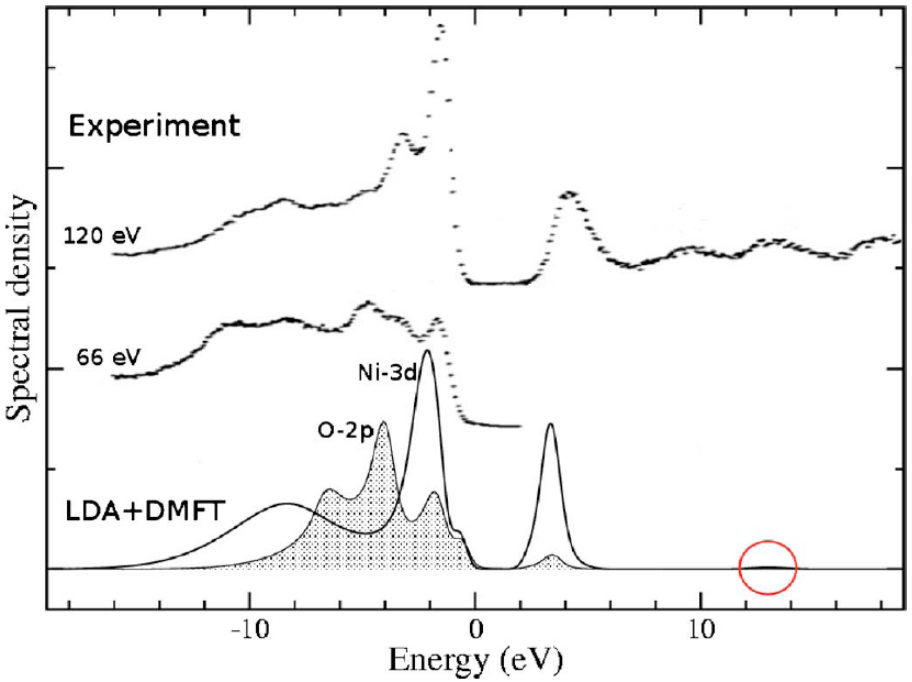


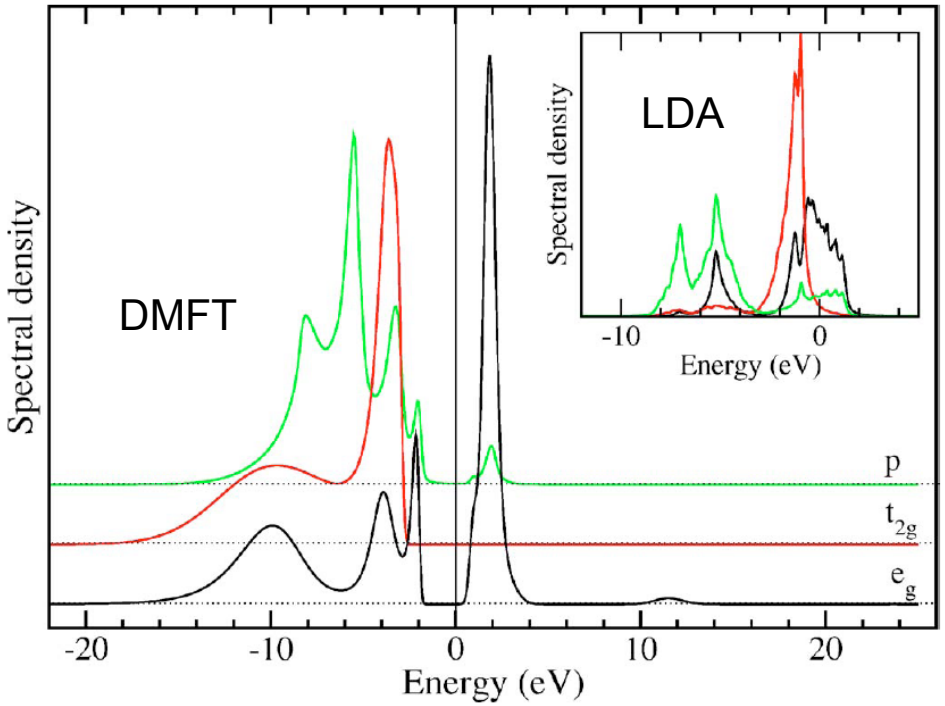


Charge transfer insulator in paramagnetic phase.
$Ni^{+2}$ ($d^8$) ion in cubic rock salt crystal structure

J. Kuneš, et al, Phys. Rev. B 75, 165115 (2007)

# Charge transfer insulator NiO

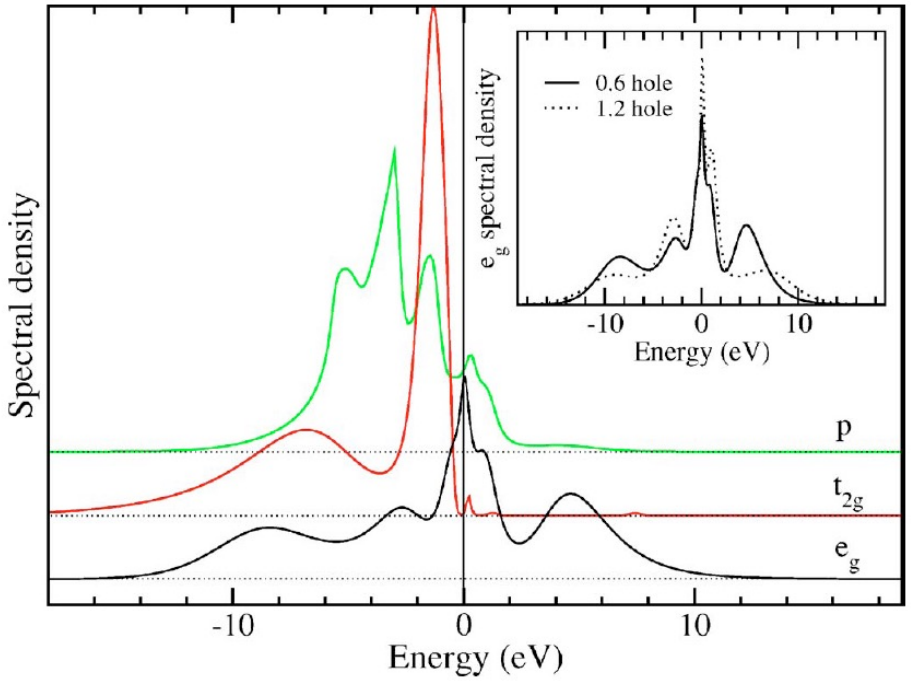


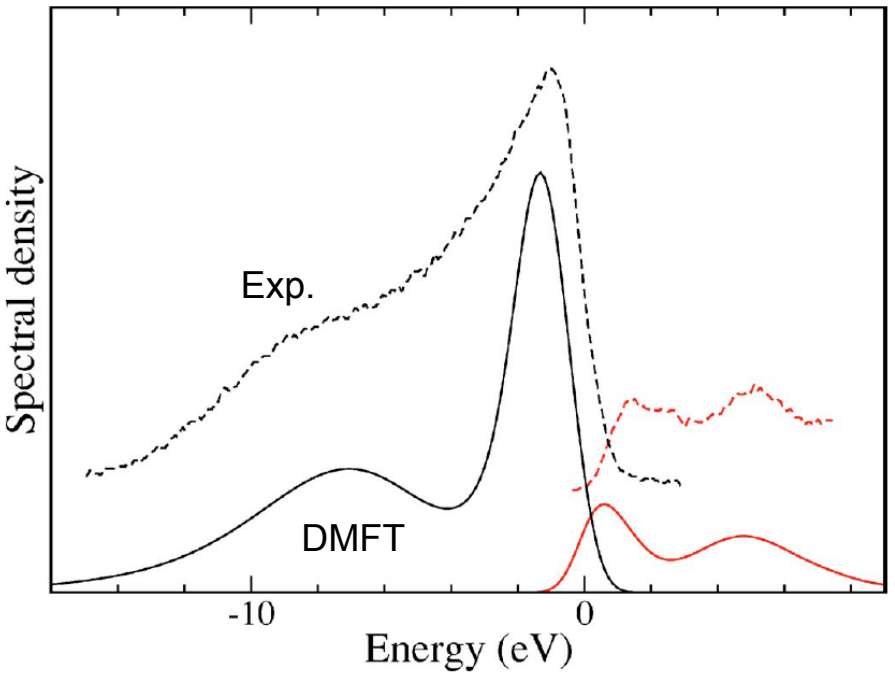


$Li_xNi_{1-x}O$ spectra

| $n_h$ | $n_{e_g}$ | $n_{t_{2g}}$ | $n_p$ | $m_d$ |
|---|---|---|---|---|
| 0 | 0.547 | 1.000 | 0.969 | 1.85 |
| 0.6 | 0.531 | 0.994 | 0.885 | 1.61 |
| 1.2 | 0.530 | 0.980 | 0.800 | 1.45 |

Holes in charge transfer insulator have predominantly oxygen 2p character.

# Charge transfer insulator NiO

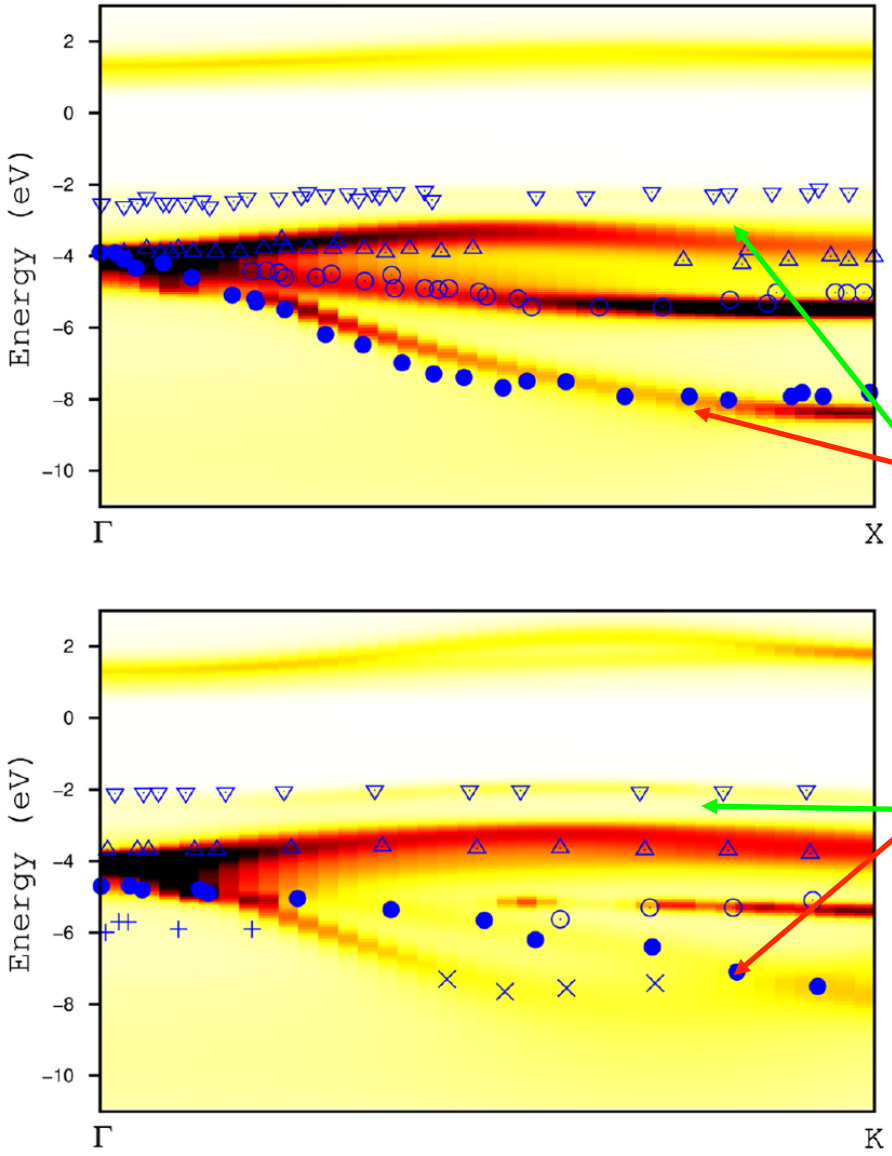


Band structure of charge transfer insulator combines dispersive (itinerant states) and flat bands (localized states).

O2p bands

Ni3d bands

J. Kunes et al, Phys. Rev. Lett. 99, 156404 (2007)

# Metal-insulator transition in MnO

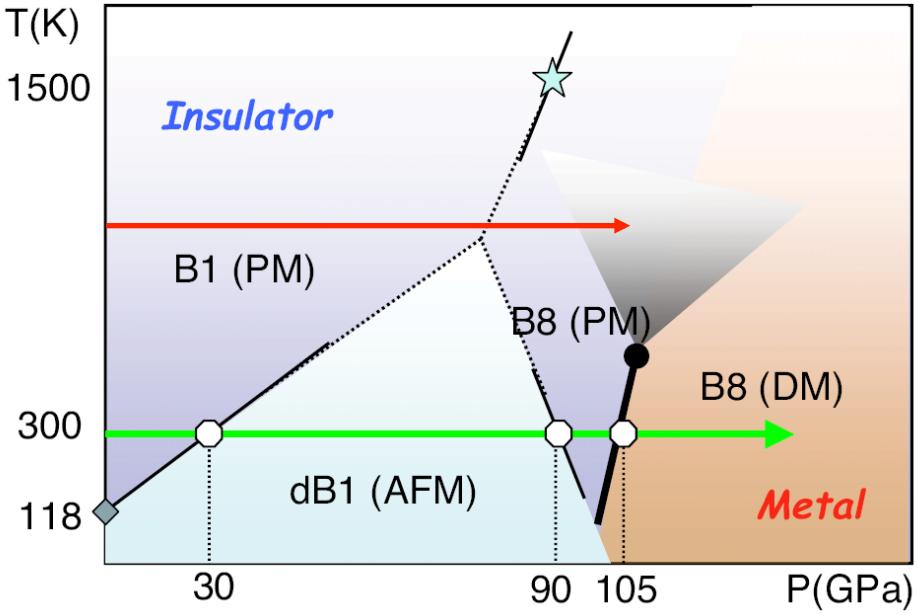


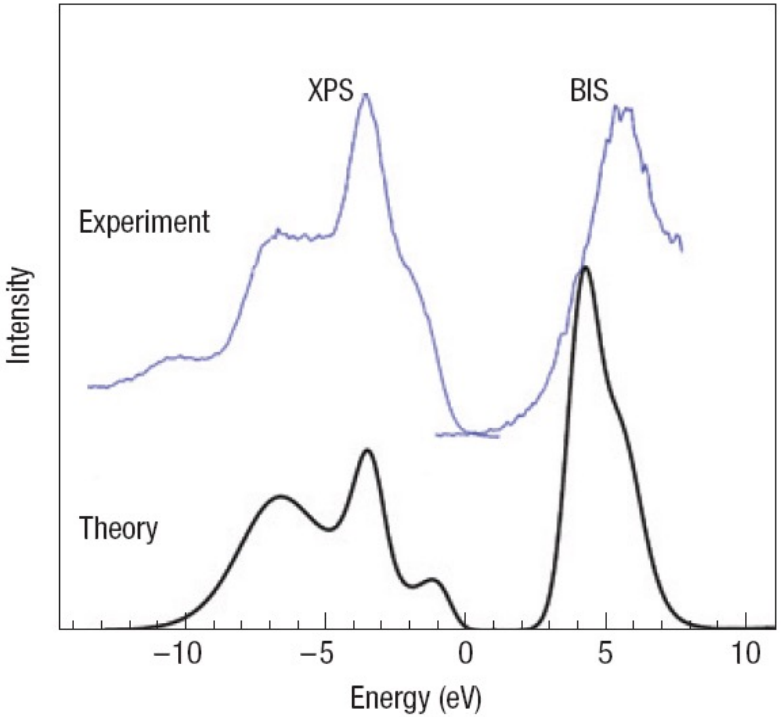


Metal-insulator transition (paramagnetic insulator to paramagnetic metal) with pressure in MnO accompanied with high-spin to low-spin state transition.

J. Kunes et al, Nature Materials 7, 198 (2008)

# Metal-insulator transition in MnO

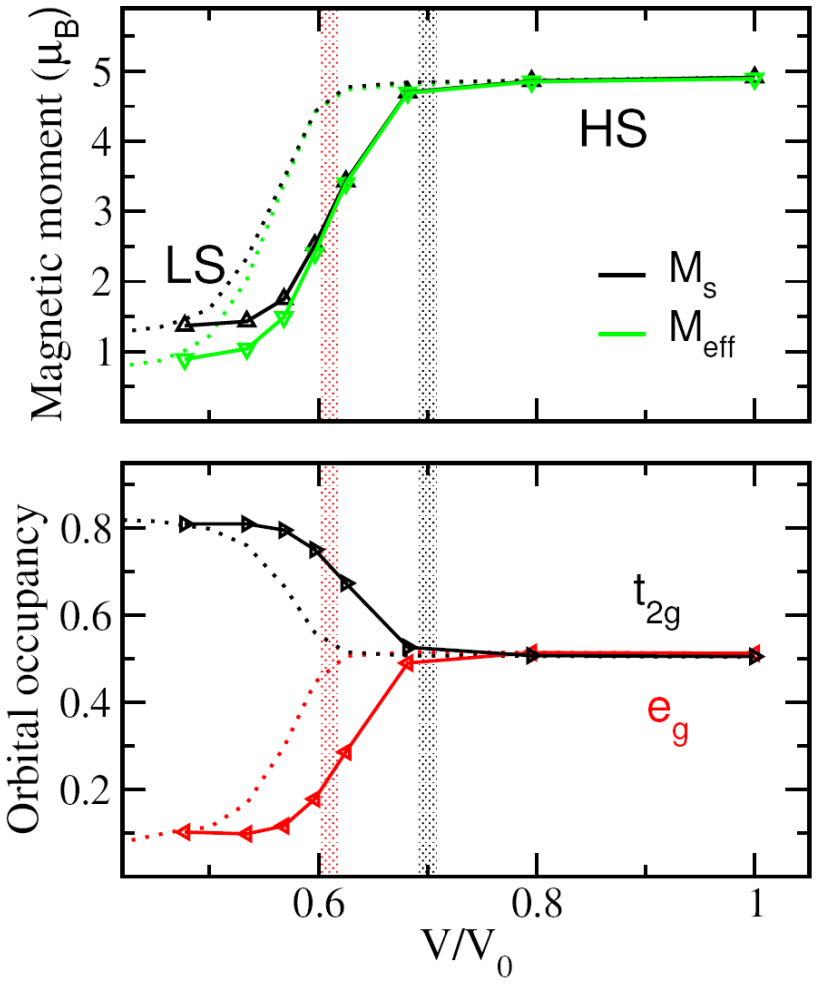


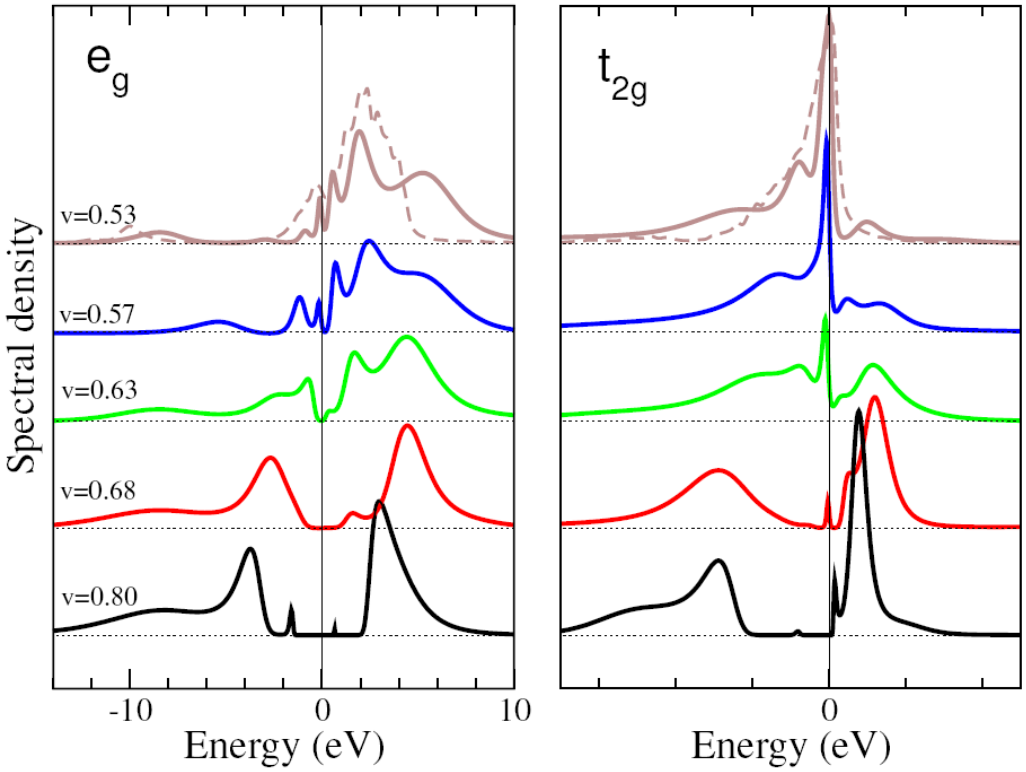


High-spin state (HS) - $t^3_{2g}\, e^2_g$ configuration

Low-spin state (LS) - $t^5_{2g}\, e^0_g$ configuration

# Metal-insulator transition in MnO

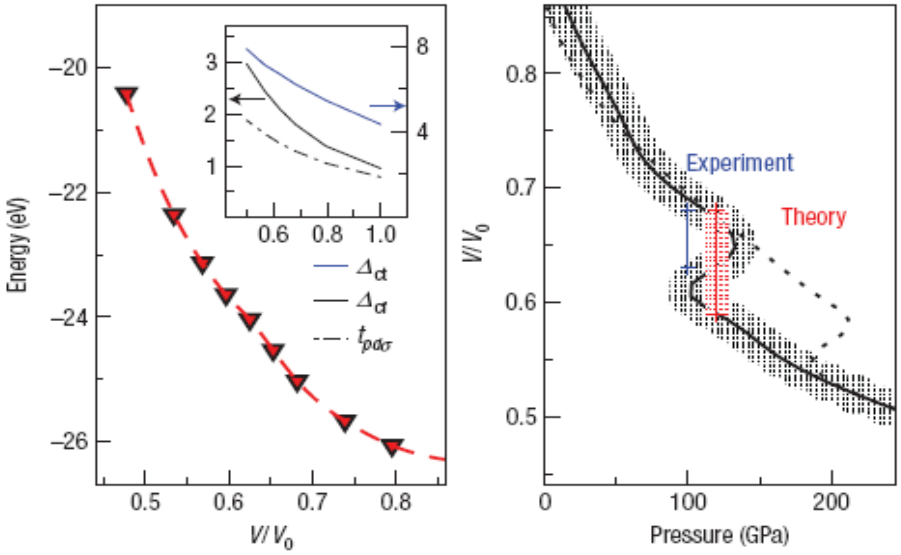


Decreasing volume with pressure increases crystal field spliting $\Delta_{cf}$ competing with exchange energy J that results in HS → LS transition with volume collapse.

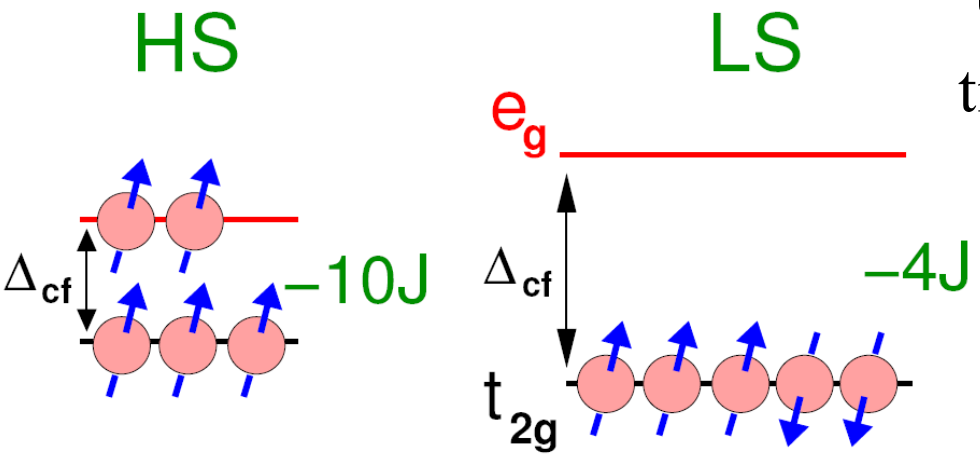

# Correlated covalent insulators FeSi and $FeSb_2$

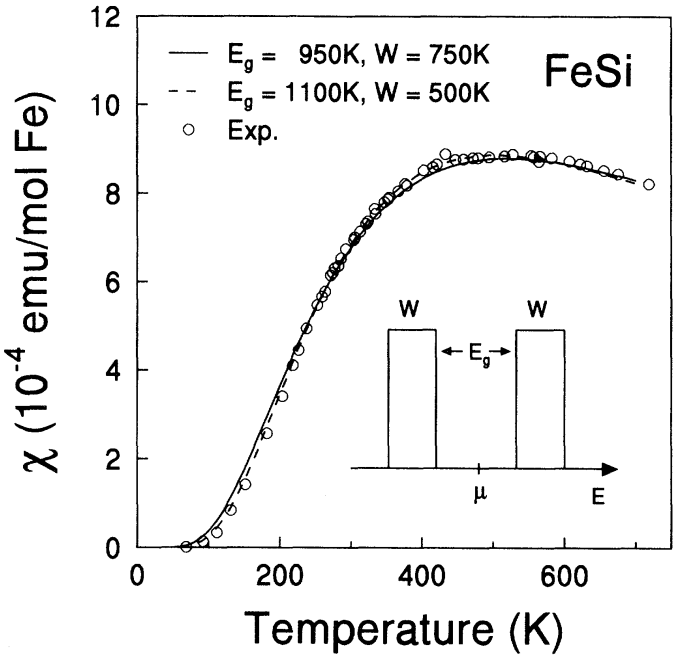


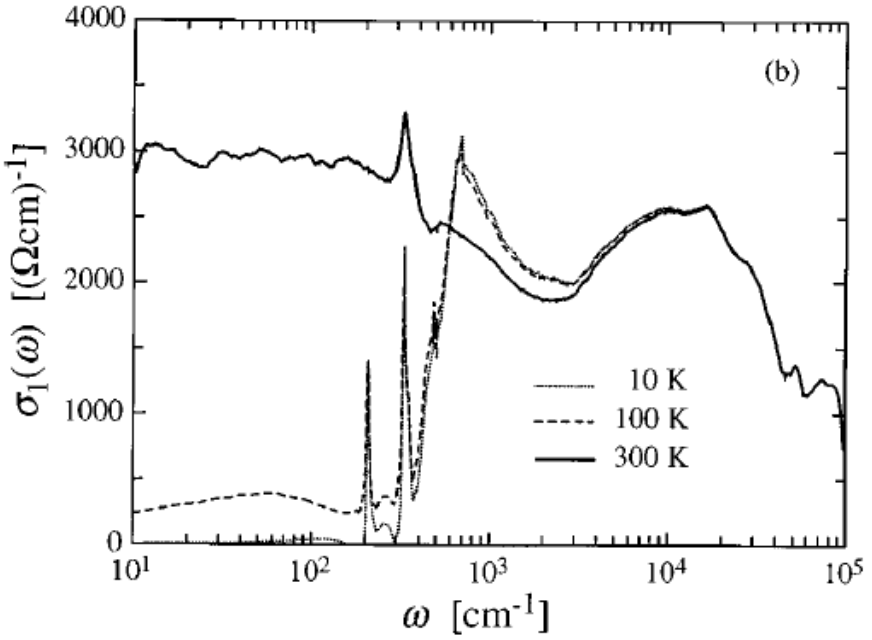


Transition from non-magnetic semiconductor to paramagnetic metal with temperature increase in FeSi and $FeSb_2$. Electron doping in $Fe_{1-x}Co_xSi$ results in ferromagnetic metallic state.

# Correlated covalent insulators FeSi and $FeSb_2$

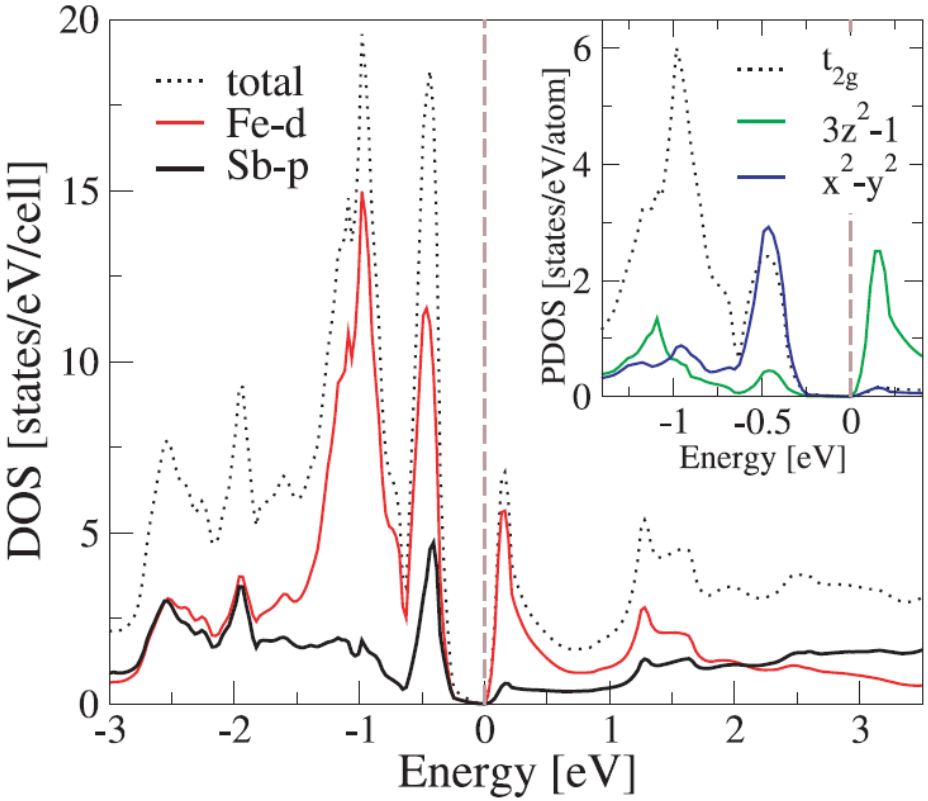


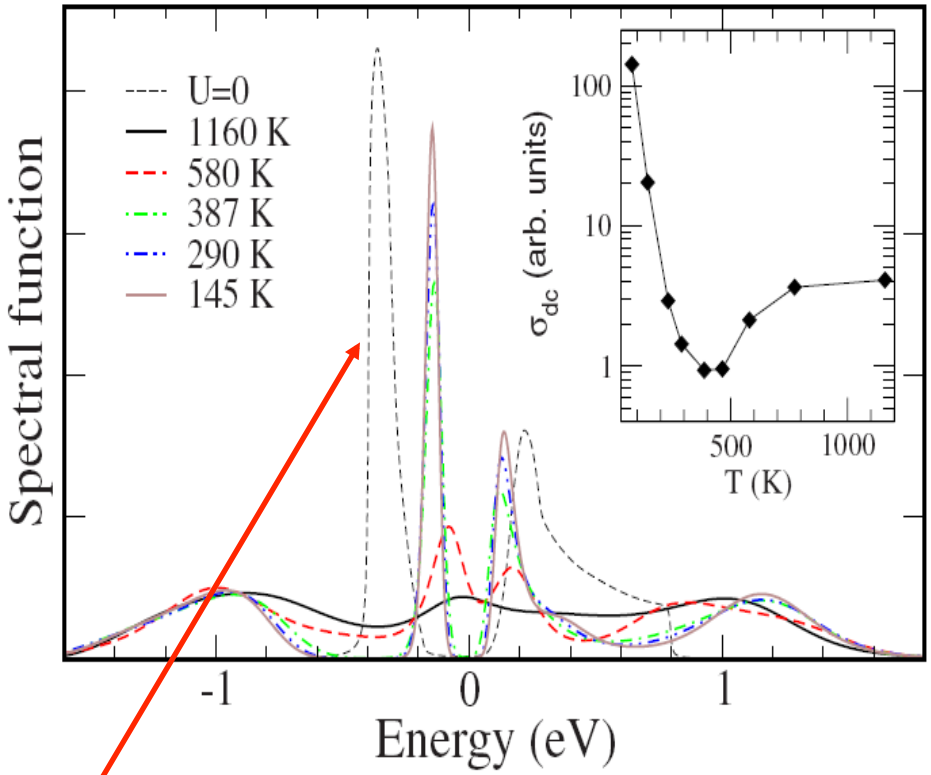


Effective one-orbital per Fe ion model corresponding to covalent insulator

J. Kunes et al, Phys.Rev. B 78, 033109 (2008)

# Correlated covalent insulators FeSi and $FeSb_2$

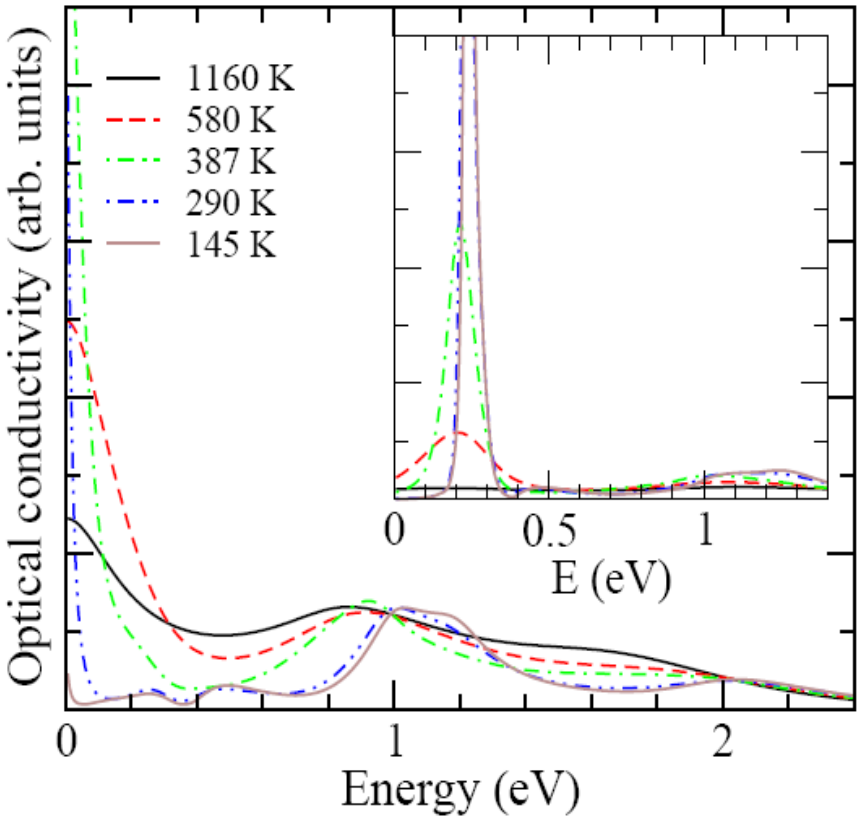


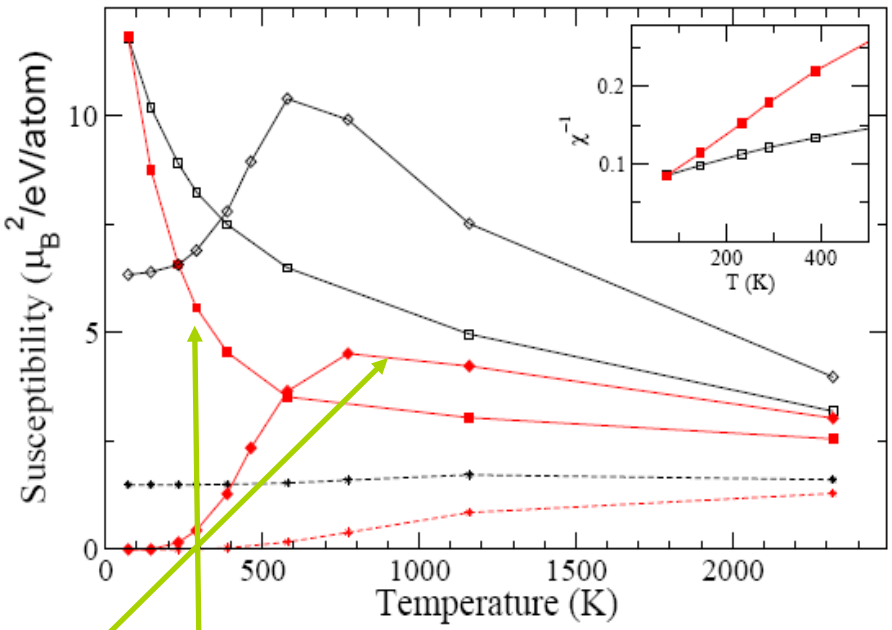


Temperature increase results in transition from nonmagnetic covalent insulator to bad metal with local moments. Electron doping leads to divergence of susceptibility for low T indicating ferromagnetic instability

# Pnictide superconductor LaOFeAs

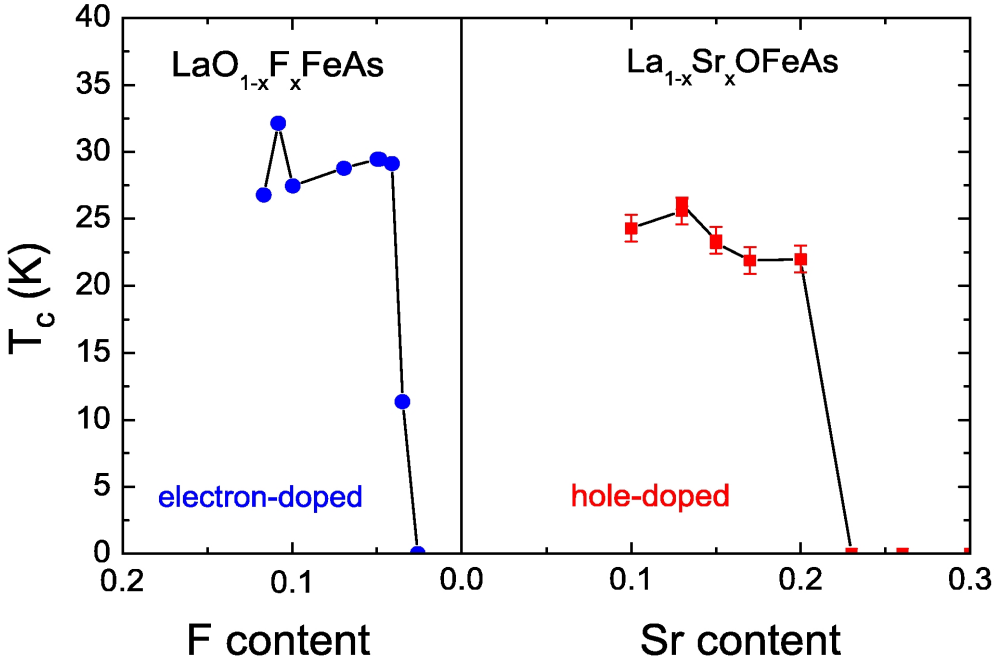


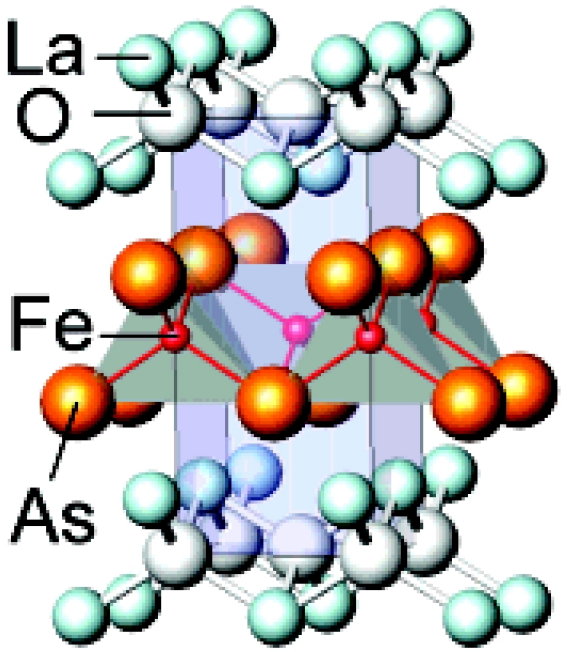


Tc=26K for F content ~11%

Y. Kanamura *et al.* J. Am. Chem. Soc. 130, 3296 (2008)]

# Pnictide superconductor LaOFeAs

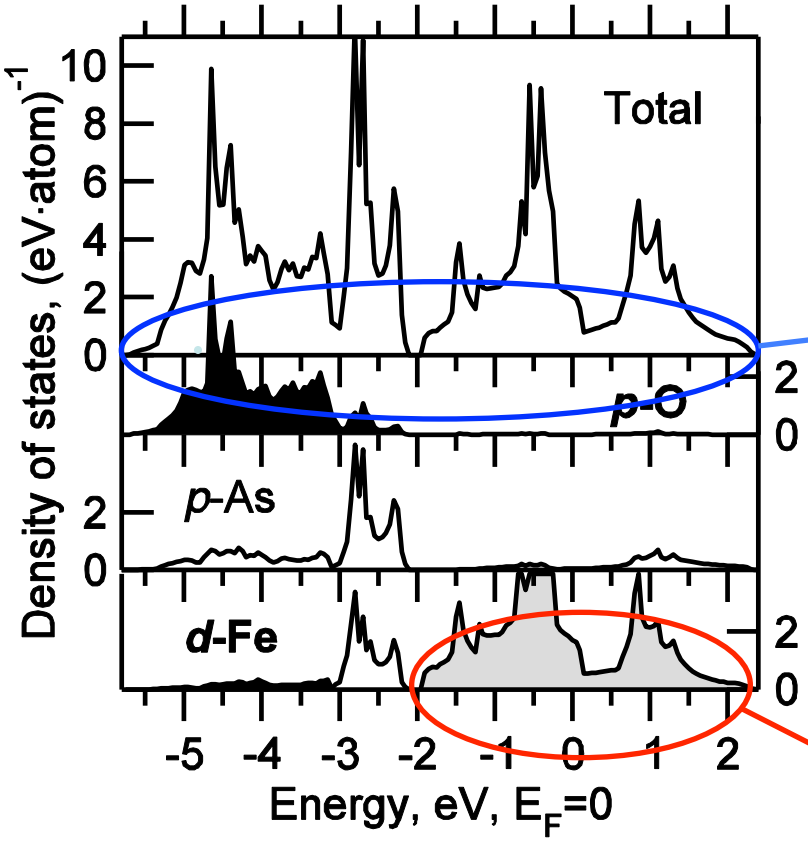


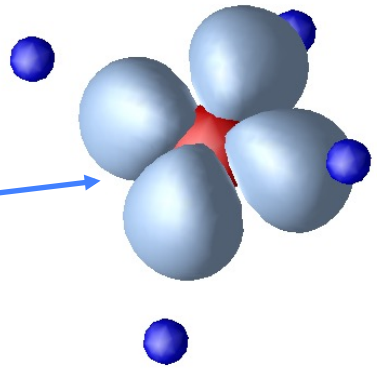

All bands WF
constrain DFT
U=3.5 eV
J=0.8 eV

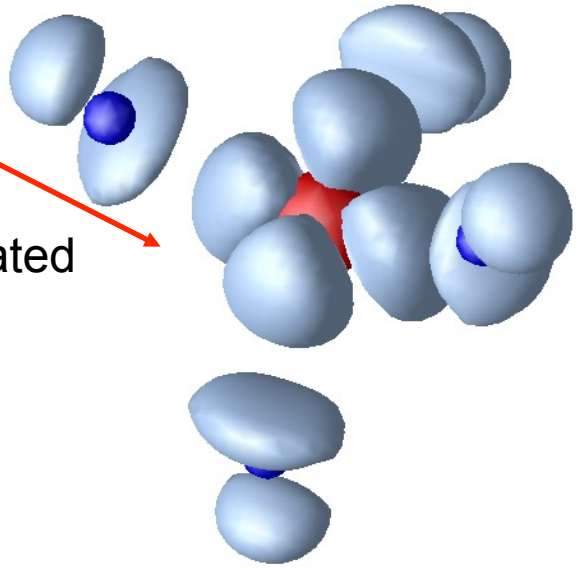

Fe3d band
only WF
constrain DFT
U=0.8 eV
J=0.5 eV

d ($x^2$-$y^2$) Wannier functions (WF) calculated
for all bands (O2p,As4p,Fe3d) and
for Fe3d bands only

V.Anisimov et al, cond-mat/0807.0547

# Pnictide superconductor LaOFeAs

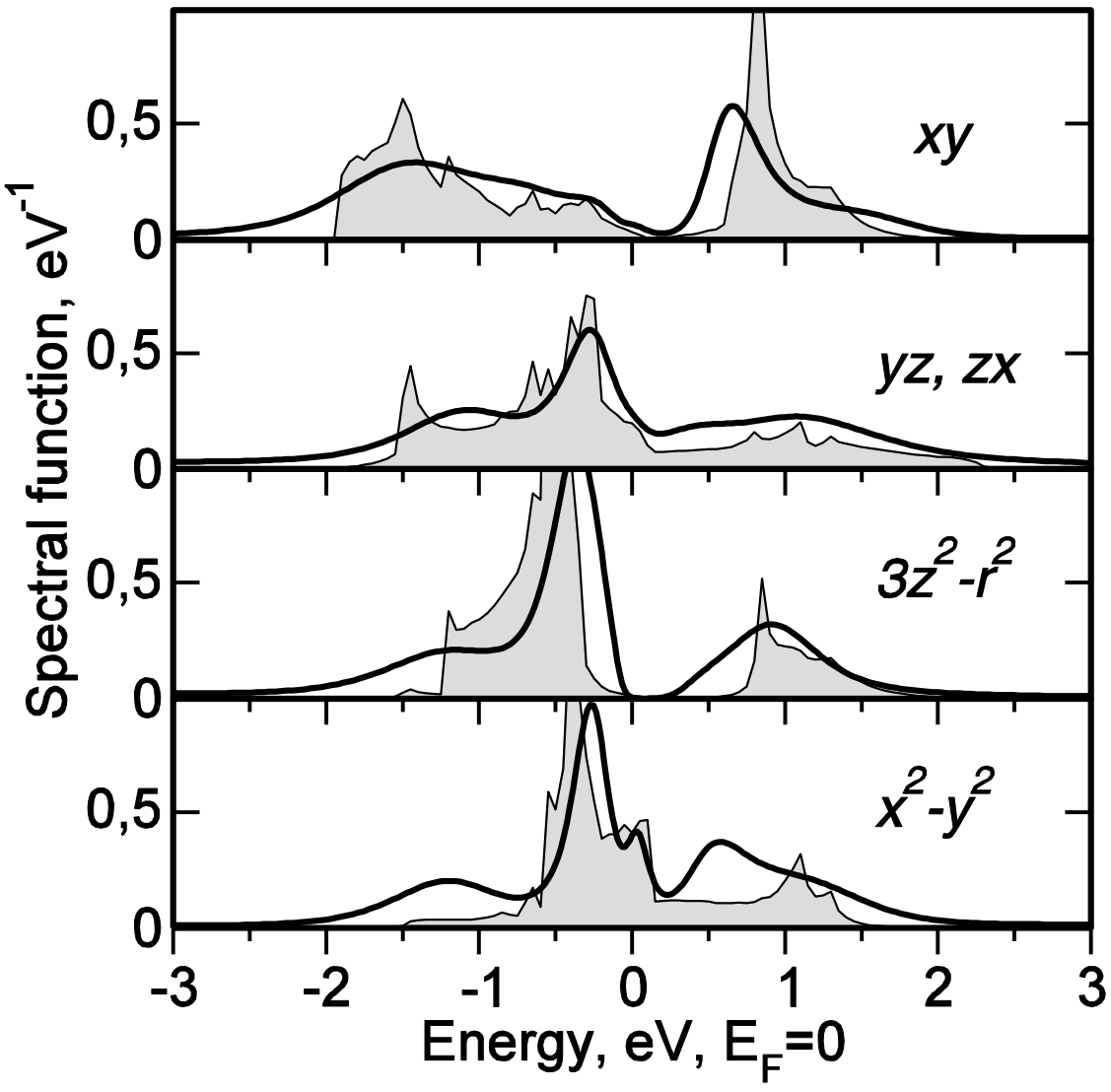


DMFT results for Hamiltonian and Coulomb interaction parameters calculated with Wannier functions for Fe3d bands only

U=0.8 eV

J=0.5 eV

*Weakly correlated regime!*

# Pnictide superconductor LaOFeAs

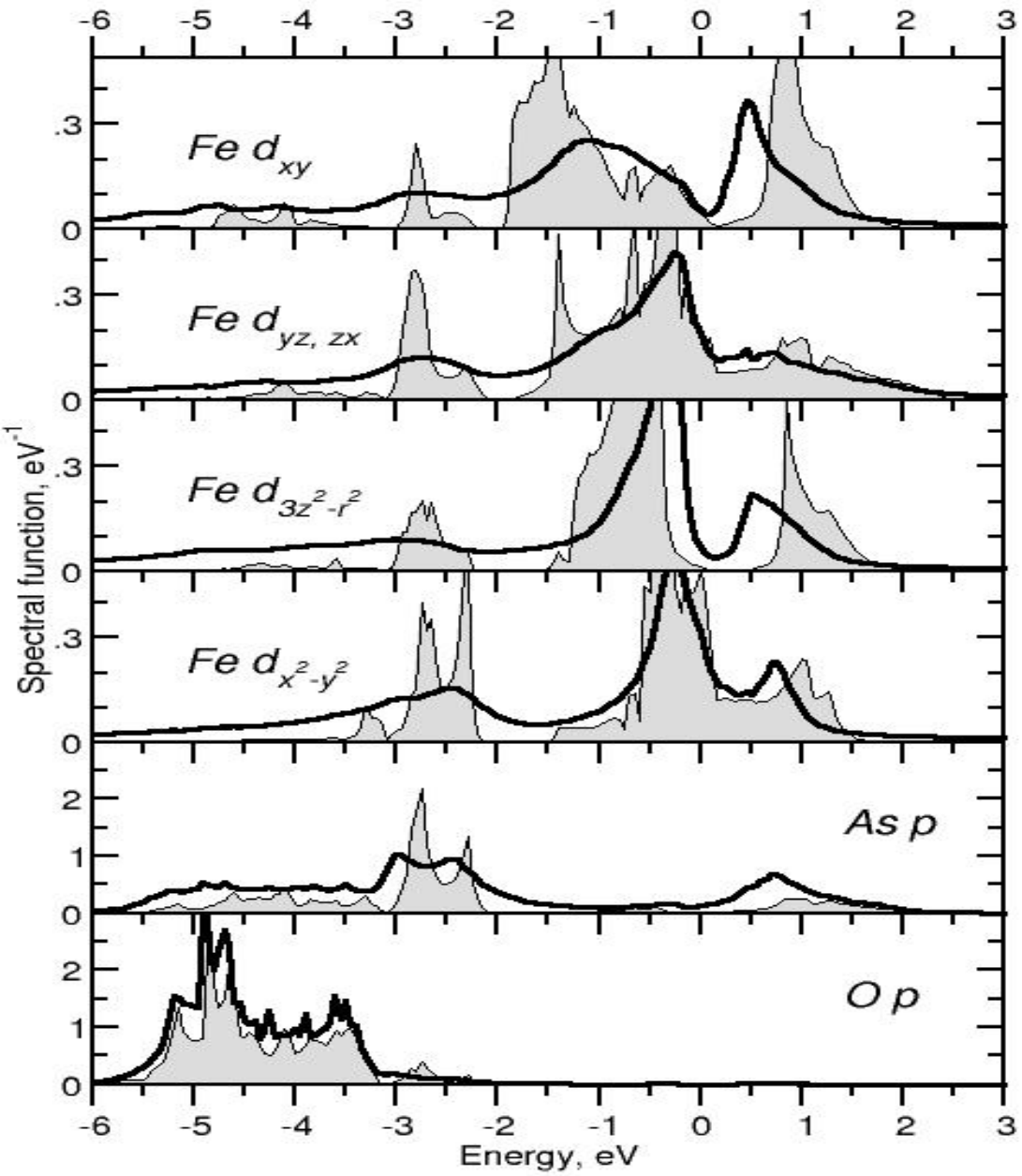


DMFT results for Hamiltonian and Coulomb interaction parameters calculated with Wannier functions
for all bands (O2p,As4p,Fe3d)
U=3.5 eV
J=0.8 eV

*Weakly correlated regime!*

# Correlations and lattice distortion: $KCuF_3$

## $KCuF_3$: a prototype $e_g$ ($3d^9$) Jahn-Teller system

Crystal structure and Orbital order (OO):

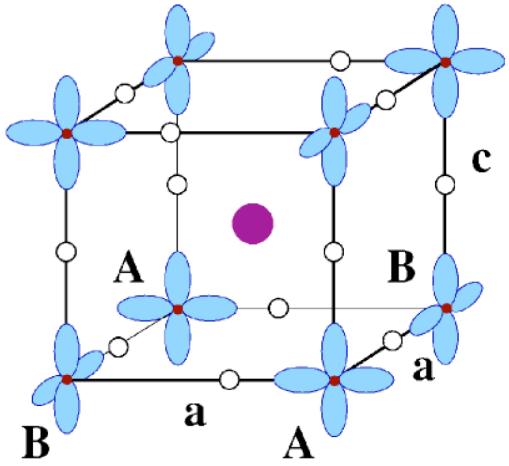


- pseudo cubic perovskite I4/mcm
- cooperative JT distortion below 1000 K
- *Neel* temperature ~38 K
- $d_{x^2-y^2}$ hole antiferroorbital ordering

d-level scheme:

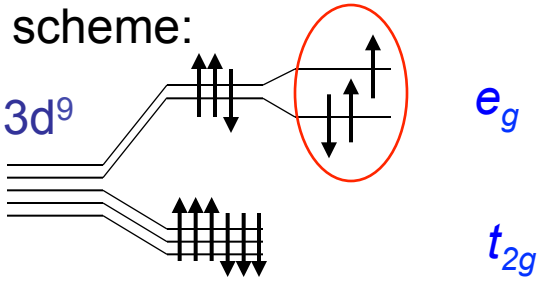


free ion cubic tetragonal ($c/a < 1$)

GGA (Cu *3d*) density of state:

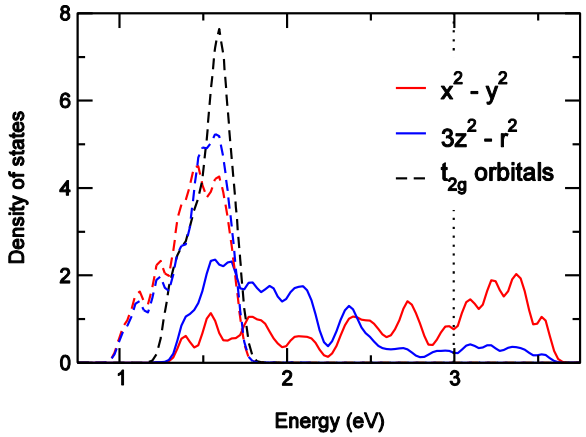


metallic solution -> inconsistent with exp

# Correlations and lattice distortion: $KCuF_3$

## $KCuF_3$: GGA+DMFT results

$U$ = 7.0 eV, $J$ = 0.9 eV

Total energy:

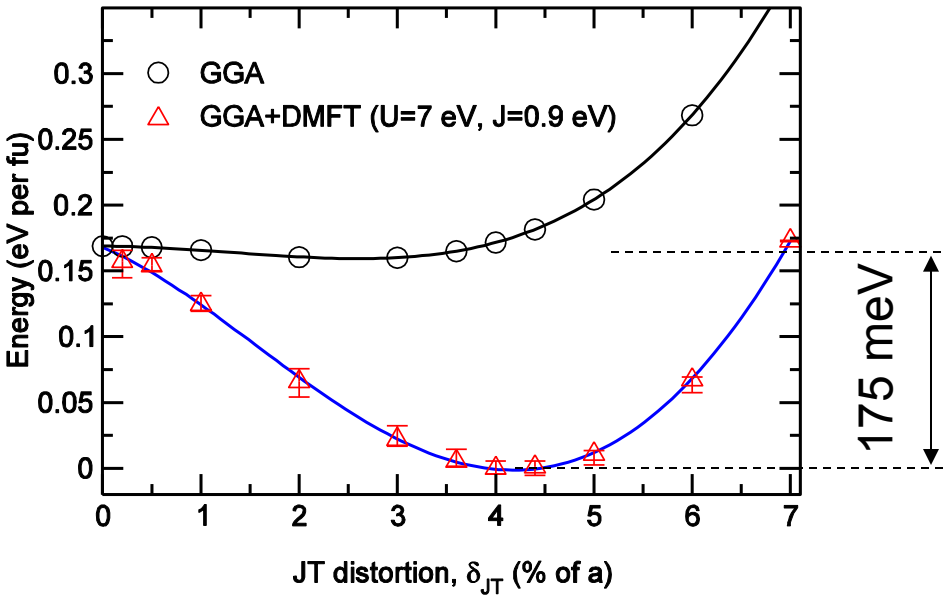


→ structural relaxation due to electronic correlations !

Leonov *et al.*, cond-mat/0804.1093, accepted to PRL

GGA:

- *metallic* solution
- total energy almost const for JT distortion < 4 %
- no JT distortion (orbital order) for T > 100 K !

→ inconsistent with experiment

GGA+DMFT:

- *paramagnetic* insulator
- energy gain of ~ 175 meV
- antiferro-orbital order
- optimal JT distortion at 4.2 %
- JT distortion persists up to 1000 K (melting tem-re)

→ in good agreement with exp

# f-electrons localization in Ce

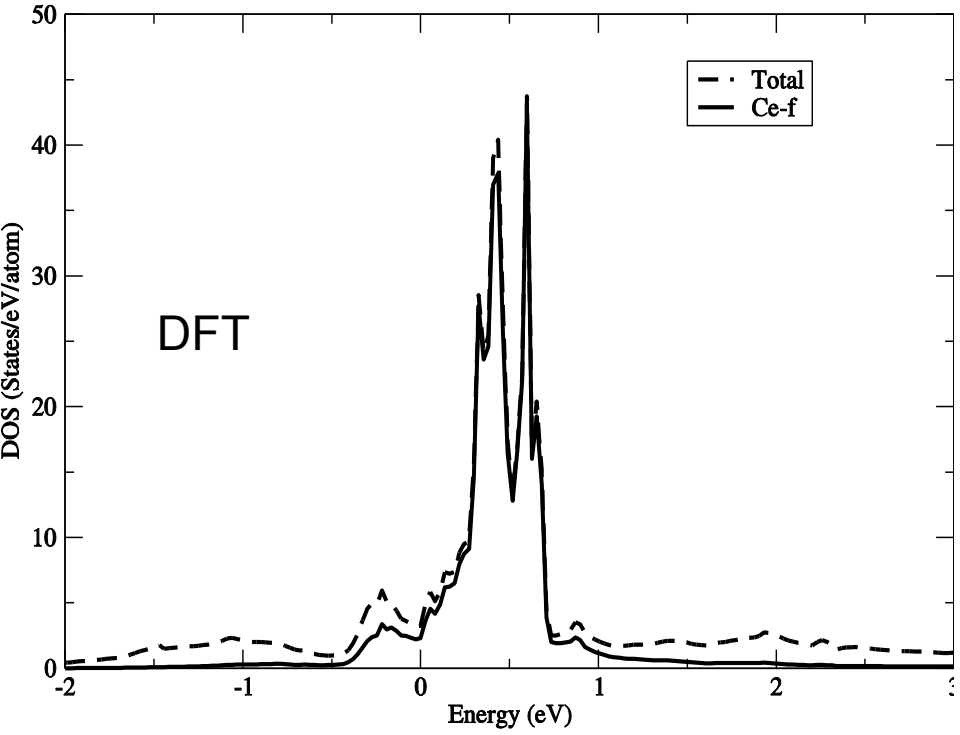


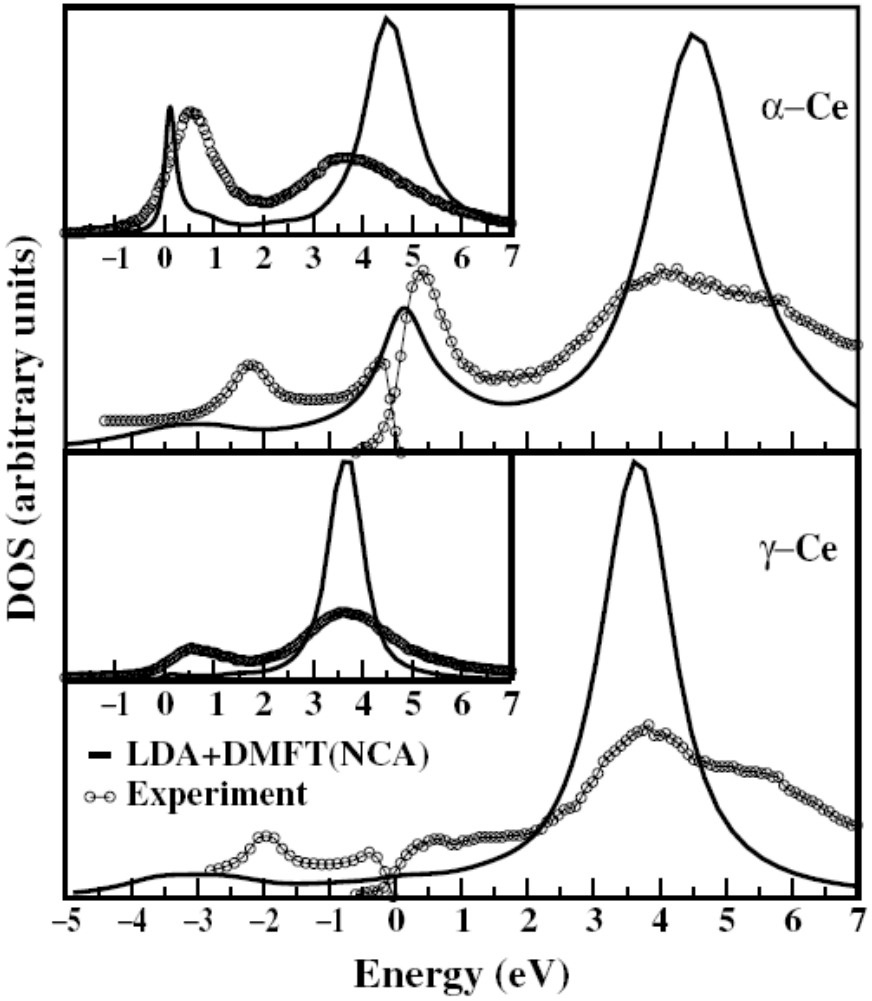


Ce a - g transition with 15% volume change.
Kondo temperature $T_K$ 1000K (a) , 30K (g)

M.B. Zoelfl et al, Phys. Rev. Lett. 87, 276403 (2001)

# Conclusions

- **Dynamical mean-field theory (DMFT) is a powerful tool to study correlation effects**
- ***Ab-initio* definition of correlated orbitals and interaction strength (U) between them based on Wannier functions formalism results in "first-principles" DFT+DMFT calculations scheme**
- **DFT+DMFT method was successful in describing paramagnetic Mott insulators, correlated metals, charge transfer insulators, metal-insulator transitions with pressure and temperature, cooperative Jahn-Teller lattice distortions**